Check for updates

New Phytologist

Resolving the contrasting leaf hydraulic adaptation of C_3 and C_4 grasses

Alec S. Baird[1,2,3], Samuel H. Taylor[4,5], Jessica Pasquet-Kok[1], Christine Vuong[1], Yu Zhang[1], Teera Watcharamongkol[5,6], Hervé Cochard[7], Christine Scoffoni[8], Erika J. Edwards[9], Colin P. Osborne[5] and Lawren Sack[1]

[1]Department of Ecology and Evolutionary Biology, University of California Los Angeles, 621 Charles E. Young Dr. South, Los Angeles, CA 90095, USA; [2]Institute of Plant Sciences, University of Bern, Altenbergrain 21, 3013, Bern, Switzerland; [3]Oeschger Centre for Climate Change Research, University of Bern, Bern, 3012, Switzerland; [4]Lancaster Environment Centre, University of Lancaster, Lancaster, LA1 4YW, UK; [5]Plants, Photosynthesis and Soil, School of Biosciences, University of Sheffield, Sheffield, S10 2TN, UK; [6]Faculty of Science and Technology, Kanchanaburi Rajabhat University, Kanchanaburi, 71190, Thailand; [7]Université Clermont Auvergne, INRAE, PIAF, 63000, Clermont-Ferrand, France; [8]Department of Biological Sciences, California State University Los Angeles, 5151 State University Dr., Los Angeles, CA 90032, USA; [9]Department of Ecology and Evolutionary Biology, Yale University, New Haven, CT 06520, USA

Author for correspondence:
Alec S. Baird
Email: alecsbaird@gmail.com

Received: *26 June 2024*
Accepted: *27 November 2024*

New Phytologist (2025) **245:** 1924–1939
doi: 10.1111/nph.20341

Key words: aridity, climate, drought tolerance, photosynthesis, Poaceae, water transport.

Summary

- Grasses are exceptionally productive, yet their hydraulic adaptation is paradoxical. Among C_3 grasses, a high photosynthetic rate (A_{area}) may depend on higher vein density (D_v) and hydraulic conductance (K_{leaf}). However, the higher D_v of C_4 grasses suggests a hydraulic surplus, given their reduced need for high K_{leaf} resulting from lower stomatal conductance (g_s).
- Combining hydraulic and photosynthetic physiological data for diverse common garden C_3 and C_4 species with data for 332 species from the published literature, and mechanistic modeling, we validated a framework for linkages of photosynthesis with hydraulic transport, anatomy, and adaptation to aridity.
- C_3 and C_4 grasses had similar K_{leaf} in our common garden, but C_4 grasses had higher K_{leaf} than C_3 species in our meta-analysis. Variation in K_{leaf} depended on outside-xylem pathways. C_4 grasses have high $K_{leaf}:g_s$, which modeling shows is essential to achieve their photosynthetic advantage.
- Across C_3 grasses, higher A_{area} was associated with higher K_{leaf}, and adaptation to aridity, whereas for C_4 species, adaptation to aridity was associated with higher $K_{leaf}:g_s$. These associations are consistent with adaptation for stress avoidance.
- Hydraulic traits are a critical element of evolutionary and ecological success in C_3 and C_4 grasses and are crucial avenues for crop design and ecological forecasting.

Introduction

The grass family (Poaceae) dominates > 40% of the Earth's terrestrial surface with 12 000 species from 800 genera, including the bulk of all crops (Beer *et al.*, 2010; McSteen & Kellogg, 2022). The photosynthetic diversity of grasses is a major factor in their dominance and in their resilience to climate change (Higgins & Scheiter, 2012). More than 40% of extant grass species have C_4 photosynthesis, which evolved > 20 times in grasses (of the > 60 times across angiosperms) and is a model for the repeated emergence of a key innovation (Gowik & Westhoff, 2011; Sage *et al.*, 2011; Grass Phylogeny Working Group II, 2012; Marazzi *et al.*, 2012), and the source of high yield in many crops and for novel varieties in development (Gowik & Westhoff, 2011; Langdale, 2011). C_4 photosynthesis maximizes carbon fixation, particularly under hotter, drier conditions or low CO_2, by concentrating CO_2 at Rubisco in the sheath around the leaf veins, minimizing photorespiratory losses, and enabling reduced stomatal conductance per leaf area (g_s) and higher light-saturated photosynthetic rate per leaf area (A_{area}) relative to g_s, resulting in higher intrinsic water use efficiency (WUE_i, that is $A_{area}:g_s$) (Supporting Information Table S1) (Sage, 2004). Yet, there has been only a fragmentary understanding of the potential contrasts in leaf hydraulic design underlying the photosynthetic and climate adaptation of C_3 and C_4 grasses, though previous work on grass leaf hydraulic design has indicated its importance in C_3 and C_4 grass performance (Ocheltree *et al.*, 2014; Baird *et al.*, 2021; Zhou *et al.*, 2021).

Generally, across plants, the leaves are bottlenecks in water transport and impose a major limitation on photosynthetic productivity (Meinzer *et al.*, 1992; Martre *et al.*, 2000; Sack & Holbrook, 2006). We extended the theory for the

© 2025 The Author(s).
New Phytologist © 2025 New Phytologist Foundation.
This is an open access article under the terms of the Creative Commons Attribution License, which permits use, distribution and reproduction in any medium, provided the original work is properly cited.

14698137, 2025, 5, Downloaded from https://nph.onlinelibrary.wiley.com/doi/10.1111/nph.20341 by Csu Los Angeles Jfk Memorial, Wiley Online Library on [29/05/2025]. See the Terms and Conditions (https://onlinelibrary.wiley.com/terms-and-conditions) on Wiley Online Library for rules of use; OA articles are governed by the applicable Creative Commons License

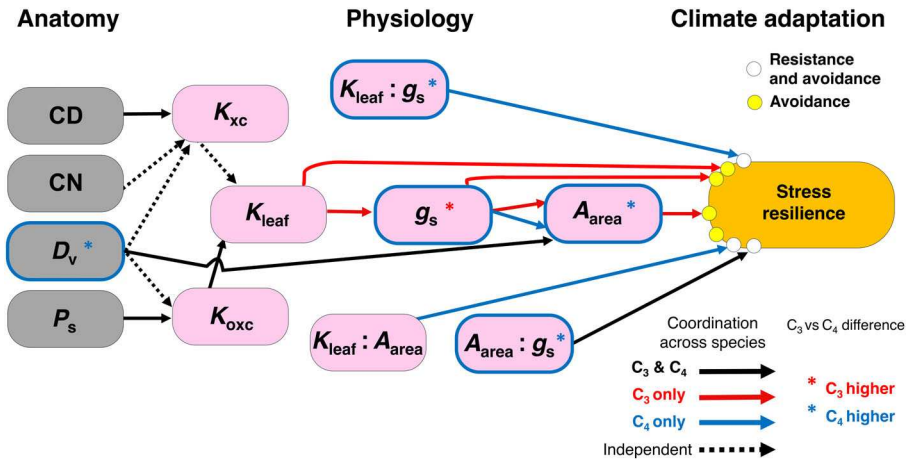

Fig. 1 Conceptual framework linking leaf anatomical, hydraulic and gas exchange traits, and their coordinated influence on adaptation to climatic aridity, supported in a common garden experiment including 27 C_3 and C_4 species. Gray and pink nodes represent anatomical and physiological traits, respectively, that contribute to drought resilience (orange node). Arrows represent relationships expected from hydraulic theory (Table 1) and supported by our experimental data. According to Hypothesis 1: a higher ratio of leaf hydraulic conductance to stomatal conductance, $K_{leaf} : g_s$ (whether driven by a high K_{leaf} or low g_s), in C_4 grasses would enable the maintenance of higher leaf water potential and g_s at lower soil water potential and/or higher vapor pressure deficit, enabling the realization of the biochemical advantage of C_4, that is, high light-saturated photosynthetic rate per leaf area (A_{area}). According to Hypotheses 2–3: among C_3 grasses, a high K_{leaf} enables a higher g_s, by maintaining high leaf water potential at a given transpiration rate and vapor pressure deficit, in turn enabling higher A_{area}. Among C_4 grasses, the disproportionately high $K_{leaf} : g_s$ leads to decoupling of K_{leaf} from g_s. According to Hypotheses 4–8: across all species, higher mean leaf vein conduit diameter (CD), conduit number (CN), and/or vein density (D_v) would contribute to higher vein xylem conduit hydraulic conductance (K_{xc}), and a higher D_v and/or vein sheath perimeter (P_s) to higher outside-xylem conduit hydraulic conductance (K_{oxc}); a higher K_{xc} or K_{oxc} would drive higher K_{leaf}. Additionally, a higher D_v may provide greater sugar transport capacity and thereby be linked with higher A_{area}. According to Hypotheses 9–10: multiple traits would contribute to drought resilience, that is, via drought resistance (the ability to maintain effective function during drought), including higher $K_{leaf} : g_s$, $K_{leaf} : A_{area}$, and $A_{area} : g_s$ for C_4 grasses; and drought avoidance (the ability to mitigate the impact of drought with high performance when moisture is available), including higher K_{leaf}, g_s, A_{area} among C_3 and higher $K_{leaf} : g_s$ and $K_{leaf} : A_{area}$ for C_4, and higher $A_{area} : g_s$ among C_3 and C_4, and thus adaptation to arid climates. Significant relationships in common garden-grown plants are depicted by solid arrows, black if significant across C_3 and C_4 species combined, red if significant for C_3 only, and blue for C_4 only; dotted lines indicate that traits that in theory (all else being equal) would contribute mechanistically to other traits, yet in this study were statistically decoupled across the studied species. Traits depicted with blue borders differed in our study on average between C_3 and C_4 species, and would contribute to the C_4 advantage; asterisks in red or blue indicate a higher value for C_3 or C_4 species, respectively. This framework is strictly conceptual and based on the hypothesized mechanisms in Table 1.

dependence of leaf gas exchange on leaf hydraulic anatomy and physiology established across diverse C_3 angiosperms (Sack & Holbrook, 2006; Brodribb *et al.*, 2007) by hypothesizing a novel general framework for the contrasting adaptation of C_3 and C_4 grasses (Fig. 1; Table 1). The premise of this theory is that water supply through the integrated leaf system needs to match evaporative demand for leaf water potential (Ψ_{leaf}) to be maintained high enough for stomata to open for photosynthetic CO_2 assimilation (Sack & Holbrook, 2006). During transpiration, liquid water moves through the network of leaf veins, which have high density (i.e. length per leaf area, D_v), and then across the bundle sheath and through the mesophyll to the sites of evaporation before diffusion from the stomata (Sack & Scoffoni, 2013), and the capacity of water transport through this system is quantified as the leaf hydraulic conductance (K_{leaf}), the ratio of transpiration rate to water potential driving force. Accordingly, across plant life forms and closely related C_3 angiosperms, hydraulics and gas exchange traits such as D_v, K_{leaf}, g_s, and A_{area} are positively coordinated (Brodribb *et al.*, 2007; Scoffoni *et al.*, 2016).

Hydraulic adaptations depend strongly on anatomy. A higher K_{leaf} can arise from a greater conductance of the xylem conduits, and/or of the outside-xylem conduit pathways (K_{xc} and K_{oxc}, respectively):

$$K_{leaf} = \left(K_{xc}^{-1} + K_{oxc}^{-1}\right)^{-1} \quad \text{Eqn 1}$$

A higher K_{xc} can be achieved through vein xylem traits, including higher conduit diameter (CD), conduit number (CN), and/or a higher D_v, which represents more parallel flow pathways. A higher K_{oxc} can also be achieved through higher D_v, shortening outside-xylem flow pathways, and also through traits that would increase vein sheath conductance (Sack & Scoffoni, 2013) (Fig. 1).

We extended hypotheses for the centrality of hydraulic adaptation in the evolution of C_4 photosynthesis in grasses. The C_4 carbon concentrating mechanism enables a higher A_{area} despite lower g_s, and higher operating Ψ_{leaf} (Osborne & Freckleton, 2009; Taylor *et al.*, 2010, 2011, 2014; Zhou *et al.*, 2021). The evolution of high photosynthetic rates in C_4 grasses depended on high D_v and enlarged mestome and/or bundle sheath cells, reducing the distance between mesophyll and sheath cells, thereby enabling the development of 'Kranz' anatomy for rapid movement of metabolites between mesophyll and sheath cells (Ogle, 2003; Sage, 2004;

© 2025 The Author(s).
New Phytologist © 2025 New Phytologist Foundation.

New Phytologist

Table 1 Framework of hypotheses for the contrasting hydraulic adaptation of C_3 and C_4 grasses, with reasoning and synthesis from previous studies.

Hypothesis	Previous work and rationale
Contrasting basis for photosynthetic diversity in C_3 and C_4 grasses, and C_4 hydraulic hyper-efficiency	
1. High photosynthetic capacity of C_3 grasses depends on high leaf hydraulic conductance (K_{leaf}), and in C_4 grasses on high K_{leaf} relative to stomatal conductance (g_s), i.e. K_{leaf} : g_s, enabling its high photosynthetic rate (A_{area}) and A_{area} : g_s (i.e. high intrinsic water use efficiency, WUE_i). A high K_{leaf} in C_3 grasses would enable high g_s and thereby higher A_{area}, whereas a higher K_{leaf} : g_s in C_4 grasses (i.e. hydraulic hyper-efficiency) would enable higher operating leaf water potential (Ψ_{leaf}), vital for realizing their higher gas exchange rates, especially necessary given the strong sensitivity of C_4 biochemistry to declining Ψ_{leaf} (Ghannoum *et al*., 2003; Osborne & Sack, 2012; Taylor *et al*., 2014; Bellasio *et al*., 2023).	In the six previous studies of hydraulic capacity in C_3 vs C_4 species of grasses or eudicots, contrasting results were reported. In three studies, K_{leaf} was similar for C_3 and C_4 grass species, that is, for studies of temperate grasses (Ocheltree *et al*., 2014), of subtropical perennial grasses (Liu *et al*., 2019) and annual grasses used as crops or their close relatives (Taylor *et al*., 2018). In two studies, K_{leaf} was higher for C_4 than C_3 grass species, that is, for studies of subtropical annual grasses (Liu *et al*., 2019) and temperate and tropical grasses, and annual and perennial grasses (Zhou *et al*., 2021). In one study, K_{leaf} was lower in C_4 *Panicum antidotale* relative to its C_3 sister taxon *P. bisulcatum* (Sonawane *et al*., 2021). In studies of C_3 and C_4 eudicots, temperate herbaceous C_4 species had lower stem hydraulic conductance (Kocacinar & Sage, 2003) as did temperate woody C_4 species (Kocacinar & Sage, 2004). In one study, temperate C_3 grass species had higher K_{leaf} than tropical C_4 species (Jacob *et al*., 2022). A high K_{leaf} : g_s enables the maintenance of g_s under atmospheric drought (i.e. high vapor pressure deficits) for temperate and tropical tree species (Brodribb & Jordan, 2008; Scoffoni *et al*., 2016). High K_{leaf} : g_s was hypothesized to enable the evolution of C_4 photosynthesis under drying conditions in a low CO_2 past (Osborne & Sack, 2012).
Contrasting coordination of hydraulic, stomatal and photosynthetic function in C_3 and C_4 grasses	
2. Across C_3 grasses K_{leaf}, g_s and A_{area} are positively coordinated. A_{area} would show a saturation response to higher g_s across C_3 grasses.	Previous studies of diverse species (Brodribb *et al*., 2007), C_3 eudicotyledons (Scoffoni *et al*., 2016), and grasses (Zhou *et al*., 2021) showed a positive coordination of hydraulics and gas exchange, that is, of K_{leaf}, stomatal conductance (g_s), and light-saturated photosynthetic rate per unit leaf area (A_{area}). The high mesophyll resistance to CO_2 diffusion in C_3 leaves would lead to saturating effects of A_{area} at high g_s (von Caemmerer & Evans, 2010).
3. Across C_4 grasses, g_s and A_{area} are decoupled from K_{leaf}. A_{area} would increase linearly with g_s across C_4 grasses.	In C_4 grasses, selection for high WUE_i, and thus, low g_s would result in a decoupling of K_{leaf} and g_s (Zhou *et al*., 2021). Decoupling of K_{leaf} and g_s was previously shown separately across 18 and nine C_4 grasses (Ocheltree *et al*., 2016; Pathare *et al*., 2020), and for K_{leaf} and A_{area} across 29 C_4 grasses (Zhou *et al*., 2021). A linear scaling of A_{area} with g_s is expected for C_4 species, which indicates a low role for mesophyll resistance in constraining photosynthetic rate (Bjorkman, 1971).
Contrasting anatomical drivers of grass leaf hydraulic function	
4. Across C_3 and C_4 grasses, variation in K_{leaf} depends on outside-xylem conduit hydraulic conductance (K_{oxc}) rather than xylem conduit hydraulic conductance (K_{xc}).	The parallel vein system of grasses, containing large xylem conduits, would provide high axial xylem transport efficiency (Givnish, 1979) such that K_{oxc} would more strongly constrain K_{leaf} across species. A large bottleneck to water transport outside the xylem was reported for nine rice genotypes (Xiong *et al*., 2017).
5. Variation in K_{xc} is driven by variation in xylem conduit diameter (CD) across C_3 and C_4 grasses.	Hydraulic conductance is highly sensitive to conduit diameter, with a 4^{th} power dependency according to the Hagen–Poiseuille equation (Nobel, 2020).
6. Across C_3 and C_4 grasses, variation in K_{oxc} is driven by variation in vein sheath properties.	A higher vein sheath perimeter represents a greater surface for exchange with surrounding mesophyll symplast and apoplast, and thus more membrane aquaporins, plasmodesmata, and cell wall transport pathways beyond suberin and lignin barriers, and would increase hydraulic conductance (Mertz & Brutnell, 2014; Sade *et al*., 2015).
7. Higher major vein density ($D_{v\text{-}major}$) and surface area per area (VSA_{major}) drive higher K_{leaf} and/or A_{area} in C_3 grasses.	$D_{v\text{-}major}$ and VSA_{major} may influence K_{oxc}, K_{leaf} and/or A_{area}. The major veins transport the bulk of leaf water throughout the leaf, given their large xylem conduits, and their larger surface for radial delivery of water to the mesophyll in transpiring leaves. These major vein traits may also correspond to greater sugar transport capacity in the phloem, and this too would be linked with higher A_{area} (Adams *et al*., 2013).
8. In C_4 species, a higher D_v would not drive a higher K_{leaf} but would drive a higher A_{area} given its representing greater allocation to vein sheath carbon assimilation tissue.	Across grasses, which have parallel major veins containing large xylem conduits, the minor vein traits (and D_v, which is related most strongly to minor vein density) would contribute minimally to the overall determination of K_{xc} or to K_{leaf}, and potentially a higher D_v would not entail substantially greater K_{xc} relative to construction costs, if it were linked with reduce conduit numbers and/or sizes. The higher minor D_v of C_4 grasses (Ueno *et al*., 2006; Baird *et al*., 2021) reflects greater allocation to vein sheaths, that is, to Kranz anatomy, and thus to carbon assimilation in sheath cells.
Contrasting adaptation of leaf hydraulics and gas exchange traits to climate in C_3 and C_4 grasses	
9. In C_3 grasses, adaptation to aridity depends on higher K_{leaf}, g_s and A_{area}.	C_3 grasses would adapt to aridity with higher hydraulic and photosynthetic rates, providing drought avoidance, that is, an ability to mitigate stressful periods by growing rapidly when water is abundant (Grubb, 1998; Volaire, 2018; Fletcher *et al*., 2022).
10. In C_4 grasses, adaptation to aridity depends on higher K_{leaf} : g_s.	C_4 grasses would adapt to aridity with a higher hydraulic supply relative to demand, providing both drought resistance, that is, an ability to maintain gas exchange when soil moisture is low, and drought avoidance, that is, growing rapidly when water is abundant (Grubb, 1998; Volaire, 2018; Fletcher *et al*., 2022).

See Supporting Information Table S1 for trait definitions and units.

© 2025 The Author(s).
New Phytologist © 2025 New Phytologist Foundation.

14698137, 2025, 5, Downloaded from https://nph.onlinelibrary.wiley.com/doi/10.1111/nph.20341 by Csu Los Angeles Jfk Memorial, Wiley Online Library on [29/05/2025]. See the Terms and Conditions (https://onlinelibrary.wiley.com/terms-and-conditions) on Wiley Online Library for rules of use; OA articles are governed by the applicable Creative Commons License

14698137, 2025, 5, Downloaded from https://nph.onlinelibrary.wiley.com/doi/10.1111/nph.20341 by Csu Los Angeles Jfk Memorial, Wiley Online Library on [29/05/2025]. See the Terms and Conditions (https://onlinelibrary.wiley.com/terms-and-conditions) on Wiley Online Library for rules of use; OA articles are governed by the applicable Creative Commons License

Ueno *et al.*, 2006; Christin *et al.*, 2013; Baird *et al.*, 2021). Yet, unlike C_3 grasses, C_4 species, once having evolved a lower g_s, may not require a higher K_{leaf} to achieve higher rates of gas exchange (Fig. 1). Indeed, for C_4 eudicots, stem hydraulic conductance was reduced relative to C_3 relatives (Kocacinar & Sage, 2003, 2004). Thus, the lack of a requirement for a high K_{leaf} in C_4 grasses poses an unresolved anatomical paradox. In C_4 grasses, the typically higher D_v associated with Kranz anatomy presents an apparent surplus of hydraulic capacity, given their reduced need for K_{leaf} due to lower g_s (Ueno *et al.*, 2006; Baird *et al.*, 2021). However, if higher D_v were coupled with fewer xylem conduits within these veins, this may negate impacts on K_{leaf}, and also indicate little carbon cost constraints to evolving higher D_v. C_4 grasses might thus be an exception to the specific trends observed across diverse plant lineages for the association between hydraulic and photosynthetic traits and their adaptation to climate. A previously proposed, but untested, hypothesis is that C_4 grasses would tend to have a higher K_{leaf} relative to g_s than C_3 species, enabling the C_4 species to maintain higher Ψ_{leaf} under mild to moderate soil or atmospheric drought that would otherwise drive declining A_{area} (Taylor *et al.*, 2011; Osborne & Sack, 2012) (Table 1). A high $K_{leaf}:g_s$ was hypothesized to enable the evolution of C_4 photosynthesis under drying conditions, especially in a low CO_2 past (Osborne & Sack, 2012), yet data have not been available to test this hypothesis. The importance of a high $K_{leaf}:g_s$ may be especially necessary given that C_4 biochemistry is highly sensitive to declining Ψ_{leaf} (Ghannoum *et al.*, 2003; Bellasio *et al.*, 2023). In contrast, we hypothesized that D_v, K_{leaf}, g_s, and A_{area} would be positively coordinated across C_3 grass species, as shown across diverse major plant lineages and across closely related angiosperms (Brodribb *et al.*, 2007; Scoffoni *et al.*, 2016).

We hypothesized that contrasting hydraulic traits of C_3 and C_4 grasses would result in differential climatic stress adaptation. Resilience to stress can depend on traits contributing to stress tolerance (i.e., maintaining growth throughout a period that includes a stress). The ability to recover after stress and, in turn, stress tolerance can be achieved through stress resistance (i.e. maintenance of function during stress), and/or avoidance (i.e. relative dormancy during stress, and maximizing growth during warm and wet periods) (Hodgson *et al.*, 2015; Volaire, 2018; Fletcher *et al.*, 2022). For C_3 grasses, high A_{area} is associated with higher g_s and transpiration rate per leaf area, and thus with high water demand, therefore requiring a higher K_{leaf} and also greater extraction of soil water. These traits would contribute to stress avoidance, that is, the maximization of assimilation under high water availability and the ability to cope with stressful periods through dormancy or an annual life cycle. By contrast, certain traits would contribute to both stress resistance and avoidance, including higher $A_{area}:g_s$ (WUE_i) and higher $K_{leaf}:g_s$, as these would enable high photosynthetic returns during dry and also moist periods, mediated by higher operating leaf water potential (Hodgson *et al.*, 2015; Volaire, 2018; Fletcher *et al.*, 2022).

We hypothesized a contrasting coordination of hydraulic, stomatal, and photosynthetic traits in C_3 and C_4 species that contributes to their ecological differentiation along a gradient of aridity. We tested a framework of hypotheses (Table 1; Fig. 1) using experimental data for >30 traits from a common experimental garden of 11 C_3 and 16 C_4 grass species, including species native to diverse habitats and major crops. With respect to phylogeny, our sample included representatives of 11 independent C_4 origins and 5 sister C_3 clades sampled within the PACMAD, as well as outgroup C_3 comparators from Oryzoideae and Pooideae (Fig. S1; Tables S1, S2). Additionally, we meta-analyzed a compiled database with data from 37 previously published studies for a total of 332 species from field studies and common garden experiments (Table S3). We elucidated the variation in K_{leaf} and its components for C_3 and C_4 grasses, their anatomical determinants, and the coordination of hydraulic and gas exchange traits with adaptation to aridity (Fig. 1; Table 1).

Materials and Methods

Plant material for experimental common garden of C_3 and C_4 grasses

We grew 27 species selected to capture large functional and phylogenetic diversity, including 11 and 16 C_3 and C_4 species, respectively, representing 11 independent C_4 origins, and five C_3 sister clades within the PACMAD (Fig. S1; Table S2), and utilized phylogenetically matched contrasts of closely related species (Funk *et al.*, 2015). Growing conditions are described in previous studies based on this experiment (Baird *et al.*, 2021, 2024) and also summarized in Methods S1. Plants were grown in a common garden design at the UCLA Plant Growth Center to reduce environmentally driven plasticity that occurs across species' distributions in the wild and thereby to better resolve genetic adaptation (Cordell *et al.*, 1998; Givnish & Montgomery, 2014; Huxman *et al.*, 2022).

We included in our analyses previously published data (Baird *et al.*, 2021, 2024) for a number of vein traits (i.e. vein diameter (VD), vein density (D_v), vein surface area per leaf area (VSA), vein projected area per leaf area (VPA), vein volume per leaf area (VVA), maximum conduit diameter (CD), leaf thickness (LT), and light-saturated photosynthetic rate per leaf area (A_{area}), as well as species-level climate data (mean annual temperature (MAT), mean annual precipitation (MAP), and mean annual aridity index (AI), i.e. MAP/potential evapotranspiration (PET)). Other hydraulic, morphological, and anatomical traits are novel to this study (described below) and were measured over the same several-month period or from tissues sampled at that time from the same plants evaluated in the previous studies (Baird *et al.*, 2021, 2024).

Sample anatomical preparation

Following the establishment of at least 3–4 mature leaves, one leaf from each of three individuals per species was fixed and stored in FAA solution (37% formaldehyde–glacial acidic acid-95% ethanol in deionized water). Leaf samples were used for creation of transverse cross sections (Methods S2).

© 2025 The Author(s).
New Phytologist © 2025 New Phytologist Foundation.

14698137, 2025, 5, Downloaded from https://nph.onlinelibrary.wiley.com/doi/10.1111/nph.20341 by Csu Los Angeles Jfk Memorial, Wiley Online Library on [29/05/2025]. See the Terms and Conditions (https://onlinelibrary.wiley.com/terms-and-conditions) on Wiley Online Library for rules of use; OA articles are governed by the applicable Creative Commons License

Quantification of leaf hydraulic traits

We measured the leaf hydraulic conductance (K_{leaf}) using the steady-state evaporative flux method (EFM) (Sack & Scoffoni, 2012), for 2–3 leaves per plant from six plants, resulting in 6–18 leaves per species (Methods S3). We determined K_{leaf} by averaging all K_{leaf} measurements for each species.

We estimated hydraulic vulnerability as the Ψ_{leaf} at 50% loss of K_{leaf} (P_{50}). For the 23 species, a linear regression fitted the data ($R^2 = 0.40$–0.88; $P < 0.001$–0.019, ordinary least squares using SMATR; Warton *et al.*, 2012), allowing identification of Ψ_{leaf} at which K_{leaf} declined to half of the *y*-intercept value. For numerous species including grasses, a straight line approximates the decline at high Ψ_{leaf} (Pasquet-Kok *et al.*, 2010; Holloway-Phillips & Brodribb, 2011; Scoffoni *et al.*, 2012).

We determined hydraulic to stomatal conductance ratio as the ratio of mean leaf hydraulic conductance relative to stomatal conductance ($K_{leaf}: g_s$).

Using K_{xc} determined by anatomical measurements (see the Quantification of vein xylem, and sheath anatomical traits subsection below), we determined K_{oxc} by re-arranging Eqn 1:

$$K_{oxc} = \left(K_{leaf}^{-1} - K_{xc}^{-1}\right)^{-1}$$

Quantification of leaf gas exchange

We measured steady-state light-saturated rates of gas exchange (< 2% change over 6 min) from 17 February to 28 June 2010, between 09:00 and 15:00 h each day, for a mature leaf on each plant for six plants per species using a LI-6400 XT portable photosynthesis system (Li-Cor, Lincoln, Nebraska, USA) (Methods S4). These measurements represented maximum rates of gas exchange, which did not differ significantly across the time of each day measured. Vapor pressure deficits (VPD) in the chamber were 0.80–1.6 kPa and the chamber was maintained at 25°C.

Quantification of vein xylem, and sheath anatomical traits

We measured and analyzed cross sections of one leaf for each of three individuals per species (Methods S5).

Vein conduit dimensions and numbers were measured for one leaf per individual for three individuals per species, in one vein of each vein order in each leaf from transverse sections imaged under a ×40 objective using a light microscope (Leica Lietz DMRB; Leica Microsystems) and camera with imaging software (SPOT Imaging Solution; Diagnostic Instruments, Sterling Heights, Michigan USA). Xylem conduits were identified by toluidine blue staining of the lignified cell walls. The theoretical conductivity (k_t; mmol m s^{-1} MPa^{-1}) was determined from Poiseuille's equation modified for ellipses (Lewis & Boose, 1995; Cochard *et al.*, 2004; Scoffoni *et al.*, 2016),

$$k_t = \frac{\pi}{64\mu}\frac{a^3 b^3}{a^2 + b^2} \quad \text{Eqn 2}$$

where μ is the viscosity of water at 25°C, and a and b are the major and minor axes of the ellipse, respectively. We measured a and b for all xylem conduits and averaged this estimate of conduit diameter for all conduits within a given vein order for each type. In grass leaves, protoxylem conduits form early within major vein orders and are destroyed during leaf expansion, which results in an empty space termed the protoxylem lacuna (Evert, 2006). We measured the dimensions of the protoxylem lacunae, as this space also transports water (Buchholz, 1921; Canny, 2001), and the wide and narrow xylem conduits (xylem type I and II, respectively) within the major veins, and the narrow xylem conduits within the minor veins (xylem II). The k_t of each longitudinal vein order was determined as the sum of the k_t of all conduits of all types:

$$1°\ k_t = 1°\ k_t \text{ Xylem I} + 1°\ k_t \text{ Xylem II} + 1°\ k_t \text{ Protoxylem Lacuna} \quad \text{Eqn 3}$$

$$2°\ k_t = 2°\ k_t \text{ Xylem I} + 2°\ k_t \text{ Xylem II} + 2°\ k_t \text{ Protoxylem Lacuna} \quad \text{Eqn 4}$$

$$3°\ k_t = 3°\ k_t \text{ Xylem II} \quad \text{Eqn 5}$$

$$4°\ k_t = 4°\ k_t \text{ Xylem II} \quad \text{Eqn 6}$$

where k_t Xylem I is the summed k_t of all type I xylem conduits, k_t Xylem II is the summed k_t of all type II xylem conduits, and k_t Protoxylem Lacuna is the k_t of the single protoxylem lacuna. This approach to the estimation of the theoretical xylem conductance (k_t) is highly standard in the field and has been used for wood (Weitz *et al.*, 2006; Alber *et al.*, 2019), veins (Sack & Frole, 2006; Pasquet-Kok *et al.*, 2010; Sommerville *et al.*, 2012; Gleason *et al.*, 2016; North *et al.*, 2016; Scoffoni *et al.*, 2016), and grasses (Martre *et al.*, 2001; Martre & Durand, 2001).

We calculated whole-leaf k_t (mmol m s^{-1} MPa^{-1}) by summing the k_t values for each longitudinal parallel vein order (Fig. 2):

$$k_t = 1°k_t + 2°k_t + 3°k_t + 4°k_t \quad \text{Eqn 7}$$

For estimating K_{xc} from vein anatomy, we applied a widely used approach (Sack & Frole, 2006; Pasquet-Kok *et al.*, 2010; Sommerville *et al.*, 2012; Gleason *et al.*, 2016; North *et al.*, 2016; Scoffoni *et al.*, 2016) (Methods S6) that has been shown to match measured K_{xc} values for grasses (Xiong *et al.*, 2017). We calculated a leaf length and area-normalized conductance of the xylem conduit lumen component of the vein system (K_{xc}, mmol m^{-2} s^{-1} MPa^{-1}) by multiplying the k_t of each vein order by its vein density (D_v, that is vein length per leaf area), which is equivalent to vein number per width for grasses, excluding transverse veins (Baird *et al.*, 2021), and then dividing by half the leaf length (LL) squared. Normalizing by LA and LL

© 2025 The Author(s).
New Phytologist © 2025 New Phytologist Foundation.

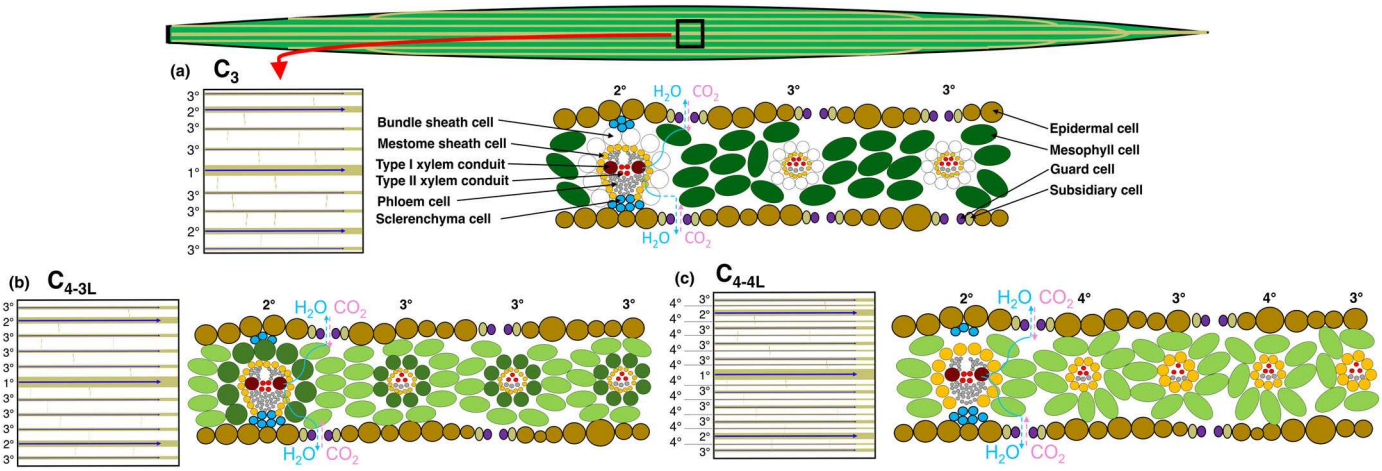

Fig. 2 Leaf hydraulic anatomy of grasses. Grasses have linearized leaves in which water flows through up to four orders of parallel longitudinal veins, including the 1° midvein and large 2° major veins, intermediate 3° minor veins and, in C_4 NADP-ME species of the subfamily Panicoideae, small 4° veins, all connected by 5° transverse veins. Water then flows outside the xylem, radially across vein sheaths, which often have hydrophobic cell walls due to suberization and/or lignification, including the mestome sheath (MS) interior to the bundle sheath (BS), and through the mesophyll, before evaporating and diffusing out of the leaf. (a) C_3 and (b) most C_4 species (i.e. $C_{4\text{-}3L}$) possess three longitudinal vein orders, whereas (c) most C_4 species of the subfamily Panicoideae evolved an additional fourth vein order, in which the MS is the only sheath (i.e. $C_{4\text{-}4L}$). Carbon reduction reactions (depicted with dark green) occur in (a) mesophyll of C_3 species, (b) in the BS of $C_{4\text{-}3L}$ species and (c) in the MS in $C_{4\text{-}4L}$ species, which is depicted in orange to differentiate the developmental origin of the MS from procambium tissue, in contrast with the BS, which derives from nonprocambium tissue (c); C_4 grasses have higher total and minor D_v, higher bundle and mestome sheath diameters (Christin *et al*., 2013), and lower stomatal densities (Taylor *et al*., 2012). The red arrow indicates a subpanel of grass leaf venation. Black arrows indicate cell types of grass leaves. Blue and pink arrows indicate water and carbon dioxide, respectively.

is necessary to scale the K_t from a conductivity to an area-specific conductance (Pasquet-Kok *et al*., 2010); using half the leaf length yields a K_{xc} representing the average vein hydraulic pathway, assuming that longitudinal veins deliver water similarly along their length, on average. K_{xc} normalized by length and area in this way is in the same units as K_{leaf}:

$$K_{xc} = \Big(\big((1° \; k_t \times 1° \; D_V) + (2° \; k_t \times 2° \; D_V) + (3° \; k_t \times 3° \; D_V) + (4° \; k_t \times 4° \; D_V)\big) \div \big(0.5 \times (LL^2)\big)\Big) \div 0.71 \quad \text{Eqn 8}$$

where 0.71 is a leaf shape area correction factor for linear leaves (Shi *et al*., 2019; Schrader *et al*., 2021).

We estimated the xylem construction cost of the major, minor, and whole vein architecture, using an index of cell wall volume per leaf area (CC; McKown *et al*., 2010).

CC for a given vein order was estimated as:

$$CC = \pi \times CD \times CN \times D_v \quad \text{Eqn 9}$$

where CD is the conduit diameter of the vein order, CN is the conduit number of the vein order, and D_v is the vein density of the vein order. For this estimation of CC, we considered xylem conduits wall thickness to be a constant (McKown *et al*., 2010). Recent work reported that, on average across woody dicot species, wider conduits have thicker (but proportionally thinner) walls (Matos *et al*., 2024); in that case, the CD term in Eqn 9 would be raised to an exponent < 1, and we considered that derivation in our interpretation.

We estimated anatomical traits as correlates of leaf outside-xylem conduit hydraulic conductance (K_{oxc}) (Methods S7). As an estimate of the surface available for flow out of the vasculature to the mesophyll, we quantified the outer perimeter of the bundle and mestome sheath (P_{bs} and P_{ms}) layers for all vein orders (Fig. 2). For each vein order, we measured the diameter of the major and minor axes of one small, medium, and large bundle and/or mestome sheath cell and averaged the major and minor axis diameters per cell, and then averaged across the cell size classes to obtain an average cell diameter. To estimate the outer perimeter, we divided this average cell diameter (D) by two and multiplied by π (i.e., representing half the perimeter of a circle) and by the number of bundle or mestome sheath cells (N) surrounding the vein of a given order and then averaged this value across all vein orders:

$$P_{bs} = (((1° D_{bs} \div 2) \times \pi \times 1° N_{bs}) + ((2° D_{bs} \div 2) \times \pi \times 2° N_{bs}) + ((3° D_{bs} \div 2) \times \pi \times 3^{\circ} N_{bs}))) \div 3 \quad \text{Eqn 10}$$

$$P_{ms} = (((1° D_{ms} \div 2) \times \pi \times 1° N_{ms}) + ((2° D_{ms} \div 2) \times \pi \times 2° N_{ms}) + ((3° D_{ms} \div 2) \times \pi \times 3° N_{ms}) + ((4° D_{ms} \div 2) \times \pi \times 4° N_{ms}))) \div 4 \quad \text{Eqn 11}$$

We also estimated the bundle and mestome sheath surface area per leaf area (BSSA and MSSA), projected area per leaf area (BSPA and MSPA) and volume per leaf area (BSV and MSV) for each vein order, and we present total BSSA and MSSA, BSPA and MSPA, and BSV and MSV (i.e., sum of all vein order

© 2025 The Author(s).
New Phytologist © 2025 New Phytologist Foundation.

14698137, 2025, 5, Downloaded from https://nph.onlinelibrary.wiley.com/doi/10.1111/nph.20341 by Csu Los Angeles Jfk Memorial, Wiley Online Library on [29/05/2025]. See the Terms and Conditions (https://onlinelibrary.wiley.com/terms-and-conditions) on Wiley Online Library for rules of use; OA articles are governed by the applicable Creative Commons License

bundle and mestome sheath surface areas, projected areas, or volumes), major BSSA and MSSA, BSPA and MSPA, and BSV and MSV (i.e., sum of major vein bundle and mestome sheath surface areas, projected areas, or volumes), and minor BSSA and MSSA, BSPA and MSPA, and BSV and MSV (i.e., sum of minor vein bundle and mestome sheath surface areas, projected areas, or volumes). We estimated the BSSA and MSSA of each vein order by first multiplying the average bundle or mestome sheath cell diameter (D) (as mentioned in the previous section) by the D_v of the vein order and by π and by the number of cells present (N), the BSPA and MSPA by multiplying the average bundle or mestome sheath cell diameter (D) (as mentioned in the previous section) by the D_v of the vein order and by the number of cells present (N), and the BSV and MSV by multiplying the square of half the average bundle or mestome sheath cell diameter (D) (as mentioned in the previous section) by the D_v of the vein order and by π and by the number of cells present (N):

$$\begin{aligned}\mathrm{BSSA} = {} & (1^{\circ}D_{\mathrm{bs}} \times \pi \times 1^{\circ}D_{\mathrm{V}} \times 1^{\circ}N_{\mathrm{bs}}) \\ & + (2^{\circ}D_{\mathrm{bs}} \times \pi \times 2^{\circ}D_{\mathrm{V}} \times 2^{\circ}N_{\mathrm{bs}}) \\ & + (3^{\circ}D_{\mathrm{bs}} \times \pi \times 3^{\circ}D_{\mathrm{V}} \times 3^{\circ}N_{\mathrm{bs}})\end{aligned} \quad \text{Eqn 12}$$

$$\begin{aligned}\mathrm{BSPA} = {} & (1^{\circ}D_{\mathrm{bs}} \times \ 1^{\circ}D_{\mathrm{V}} \times 1^{\circ}N_{\mathrm{bs}}) \\ & + (2^{\circ}D_{\mathrm{bs}} \times \ 2^{\circ}D_{\mathrm{V}} \times 2^{\circ}N_{\mathrm{bs}}) \\ & + (3^{\circ}D_{\mathrm{bs}} \times \ 3^{\circ}D_{\mathrm{V}} \times 3^{\circ}N_{\mathrm{bs}})\end{aligned} \quad \text{Eqn 13}$$

$$\begin{aligned}\mathrm{BSV} = {} & \left((1^{\circ}D_{\mathrm{bs}} \div 2)^2 \times \ 1^{\circ}D_{\mathrm{V}} \times 1^{\circ}N_{\mathrm{bs}}\right) \\ & + \left((2^{\circ}D_{\mathrm{bs}} \div 2)^2 \times \ 2^{\circ}D_{\mathrm{V}} \times 2^{\circ}N_{\mathrm{bs}}\right) \\ & + \left((3^{\circ}D_{\mathrm{bs}} \div 2)^2 \times \ 3^{\circ}D_{\mathrm{V}} \times 3^{\circ}N_{\mathrm{bs}}\right)\end{aligned} \quad \text{Eqn 14}$$

MSSA, MSPA, and MSV were calculated as in Eqns 12–14, swapping D_{bs} with D_{ms} and N_{bs} with N_{ms}, and including the 4° veins.

Compilation of grass leaf hydraulic and photosynthetic data from the literature

To characterize C_3 and C_4 differences in leaf hydraulic and photosynthetic physiology based on the previous literature, we compiled data from published studies after searching for 'grass' coupled with 'leaf physiology', 'functional trait', 'hydraulics', and 'gas exchange' (Google Scholar and Web of Science). We extracted data for 332 grass species from 37 published studies that included data for the following traits for grasses: light-saturated leaf photosynthetic rate per leaf area (A_{area}), stomatal conductance (g_s), leaf hydraulic conductance (K_{leaf}), leaf xylem conduit hydraulic conductance (K_{xc}), leaf outside-xylem hydraulic conductance (K_{oxc}), vein density (D_v), intrinsic leaf water use efficiency (WUE_i), leaf water potential at turgor loss point (TLP), leaf water potential at 50% loss of leaf hydraulic conductivity (P_{50}), and leaf water potential at 80% loss of leaf hydraulic conductivity (P_{80}) (Table S3). Traits were averaged for species included in several studies. For studies that included data for K_{leaf} and g_s at the species level, we estimated the ratio of K_{leaf} : g_s.

Modeling the native climate of C_3 and C_4 grass species

Modeled climate variables were obtained by averaging climate across each species distribution under the assumption that mean phenotypic trait values per species would be indicative of their mean climate variables if gene flow occurs among populations of each species (Sexton *et al.*, 2009). Additional details on these methods are provided in a previous publication (Baird *et al.*, 2021) and in Methods S8.

Statistical analyses: phylogenetic comparative methods

We utilized a phylogenetic approach to account for the influence of phylogenetic covariance on average C_3 and C_4 trait differences and on trait–trait relationships using the R Language and Environment (R Core Team, 2023). For analyses including the 27 species grown in a common garden, we utilized a previously published time-calibrated phylogeny (Baird *et al.*, 2021). For the compiled grass database, we implemented phylogenetic analyses to test differences in traits between C_3 and C_4 species, and to test relationships between traits for all grasses, C_3 grasses only, and C_4 grasses only. As each trait in the larger database had a different sample size, we used numerous different phylogenies, depending on the species set, to test for trait differences or trait–trait relationships, each trimmed from a larger global grass phylogeny (Spriggs *et al.*, 2014).

Our analyses utilized a custom-written code that is available on GitHub (https://github.com/smuel-tylor/grass-leaf-size). For analyses of the 27 species from the common garden, and for the 332 species from the compiled database, we examined differences in species-level trait means between C_3 and C_4 species using a phylogenetically corrected analysis of variance (ANOVA), both parametric (based on PGLS) and nonparametric (Garland *et al.*, 1993) using the PHYLOANOVA package (Revell, 2012). We also tested for relationships between leaf gas exchange and leaf structure, climate, and between leaf hydraulic traits and leaf hydraulic anatomy using phylogenetically corrected regressions, including reduced major axis regressions (PRMA) or generalized least square regressions (PGLS), which incorporate phylogenetic correction as Pagel's λ (Pagel, 1999; Freckleton *et al.*, 2002) estimated by maximum likelihood (Pinheiro *et al.*, 2019) (Methods S9).

We implemented both phylogenetic and nonphylogenetic tests for analyses of trait–trait relationships across the 332-species database. The phylogenetic tests resulted in reduced coverage of the trait space and particular C_3 and C_4 clades being disproportionately sampled, as many of the phylogenies generated for each trait–trait relationship could not account for all of the species in the database, due to species not being present in the larger phylogeny (Spriggs *et al.*, 2014) (see Methods S9 for details). Thus, we present both phylogenetic and nonphylogenetic analyses, but emphasize the nonphylogenetic analyses for our findings on trait–trait relationships for the 332 species. We used the function cor.test to test for significant correlations between traits and present the Pearson correlation coefficient, r, and statistical significance P-value. The

© 2025 The Author(s).
New Phytologist © 2025 New Phytologist Foundation.

14698137, 2025, 5, Downloaded from https://nph.onlinelibrary.wiley.com/doi/10.1111/nph.20341 by Csu Los Angeles Jfk Memorial, Wiley Online Library on [29/05/2025]. See the Terms and Conditions (https://onlinelibrary.wiley.com/terms-and-conditions) on Wiley Online Library for rules of use; OA articles are governed by the applicable Creative Commons License

14698137, 2025, 5, Downloaded from https://nph.onlinelibrary.wiley.com/doi/10.1111/nph.20341 by Csu Los Angeles Jfk Memorial, Wiley Online Library on [29/05/2025]. See the Terms and Conditions (https://onlinelibrary.wiley.com/terms-and-conditions) on Wiley Online Library for rules of use; OA articles are governed by the applicable Creative Commons License

studies included in the meta-analysis are provided in Table S3 and the Supporting Information reference list.

Modeling of hydraulic–stomatal–photosynthetic function of C_3 and C_4 species under varying levels of soil and atmospheric drought

We used the mechanistic hydraulic model SurEau v. 2021-11-10 (Cochard *et al.*, 2021) to simulate the impact of soil drought on the water relations and gas exchange of representative C_3 and C_4 plants (Methods S10). We parameterized the photosynthesis model for C_3 plants (von Caemmerer, 2000, 2021; Osborne & Sack, 2012; Bonan, 2019) and C_4 (Yin *et al.*, 2011; von Caemmerer, 2021), using average values for physiological traits taken from our experiment or others published previously (Table S4). The plant's total hydraulic conductance was adjusted to obtain the operational leaf water potential value for each plant type.

The dependence of stomatal conductance (g_s) and leaf hydraulic conductance (K_{leaf}) on leaf water potential (Ψ_{leaf}) were modeled as:

$$g_s = \frac{g_{max}}{1 + \exp\left(\frac{\Psi_{leaf} - \Psi_{gs50}}{c}\right)} \quad \text{Eqn 15}$$

where g_{max} is the maximal stomatal conductance, Ψ_{leaf} is the leaf water potential, Ψ_{gs50} is the leaf water potential at 50% stomatal closure, and c is a constant, and

$$K_{leaf} = K_{max} + a \times \Psi_{leaf} \quad \text{Eqn 16}$$

where K_{max} is the maximum leaf hydraulic conductance and a is the mean slope for K_{leaf} vs Ψ_{leaf}. For the simulations, we tested hydraulic and photosynthetic responses to declining soil water potential under two VPDs: 0.5 and 3 kPa. Thus, 0.5 kPa VPD was implemented by setting the maximum temperature to 20°C and minimum relative humidity to 78.6%, and the 3 kPa VPD by setting the maximum temperature to 30°C and minimum relative humidity to 29.5%. The simulation starts with soil at field capacity and is allowed to gradually dehydrate under the influence of plant transpiration.

To test the influence of K_{leaf} : g_s on the drought response of gas exchange, in addition to simulating C_3 and C_4 grasses, we also simulated a C_3 grass with the average K_{leaf} : g_s of C_4 species, and a C_4 grass with the average K_{leaf} : g_s of C_3 species (Table S4).

Results

Leaf hydraulic transport in grasses and C_4 hydraulic hyperefficiency

In our meta-analysis, C_4 grass species had a 1.4-fold higher K_{leaf} and a twofold higher K_{leaf} : g_s than C_3 species (Fig. 3a; Tables S2, S3). We also found differences between C_3 and C_4 species consistent with our hypotheses and the previous literature (Table 1). In the meta-analysis, C_4 grasses had 1.6- to 2.2-fold higher A_{area}, WUE_i, and D_v, and 71% lower g_s (phylogenetic ANOVA; Fig. 3a; Tables S2, S3). Furthermore, in our compiled database, C_3 and C_4 grass species were statistically similar in their hydraulic sensitivity to drought, that is, their leaf hydraulic vulnerability to decline of Ψ_{leaf} ($P_{50} = \Psi_{leaf}$ at 50% loss of K_{leaf}) and leaf turgor loss point (TLP = Ψ_{leaf} at turgor loss). In our common garden, K_{leaf}, K_{xc}, and K_{oxc} did not differ on average between the C_3 and C_4 terrestrial species, and the C_4 species had a twofold higher K_{leaf} : g_s and a higher operating Ψ_{leaf} (Table S2). Notably, phylogenetic and ahistorical tests showed similar results for average C_3 and C_4 trait differences and regression analyses (Tables S3, S5).

The importance of high K_{leaf} : g_s in realizing the C_4 photosynthetic advantage was demonstrated by our integrated whole-plant modeling of the grass photosynthetic, stomatal, and hydraulic systems (Figs 3b–d, S2). For Ψ_{soil} values representing moist to moderately dry soil, C_4 species maintained higher modeled Ψ_{leaf} values than C_3 species, and a superior ability to maintain g_s and A_{area}. When simulating a C_4 grass with the lower K_{leaf} : g_s that was quantified for C_3 grasses (by reducing K_{leaf} proportionately with the lower g_s of C_4 species) Ψ_{leaf} and g_s declined steeply with reduction in Ψ_{soil} and the C_4 advantage of high A_{area} was lost at mild levels of drought. A simulated C_3 grass with higher K_{leaf} : g_s (i.e. that observed in C_4 species, achieved by increasing K_{leaf}) had higher Ψ_{leaf} and moderately higher g_s or A_{area}.

Coordination of hydraulic, stomatal, and photosynthetic function in grasses

The C_3 and C_4 grasses showed contrasting coordination of K_{leaf}, g_s, and A_{area} in both our compiled database and in the 27 species common garden (Figs 4, 5; Tables S5, S6). Among the C_3 grasses in the common garden, and in the compiled database, A_{area} and g_s scaled with K_{leaf} (Figs 4a, 5a; Tables S5, S6). C_4 grasses showed no association of gas exchange with hydraulic traits, with low g_s and moderate to high A_{area} across the range of K_{leaf}, relative to C_3 species (Figs 4a, 5b,c; Table S5). C_3 and C_4 species differed in the relationship of A_{area} to g_s (Figs 4b, 5a). Among C_3 species, while A_{area} initially increased with g_s, at high g_s beyond *c.* 0.4 mol m^{-2} s^{-1} there were slight gains in A_{area}. Among C_4 species, there was a steeper relationship, shifted toward a higher A_{area} at a given g_s and without evidence of saturation at high g_s.

Anatomical drivers of grass leaf hydraulic and photosynthetic function

We examined the anatomical drivers of grass leaf hydraulic and photosynthetic capacity across the 27 diverse C_3 and C_4 common garden-grown species (Fig. 6; Tables S5, S7, S8). K_{leaf}, K_{xc}, and K_{oxc} were related to A_{area} and vascular anatomy (Tables S6, S7).

Among C_3 and C_4 grass species, variation in K_{leaf} was independent of K_{xc}, and related to variation in K_{oxc} (Fig. 6a). Among C_3 and C_4 species, K_{oxc} and K_{leaf} increased positively with the outer perimeter of the bundle and mestome sheaths (P_{bs} and P_{ms}; Fig. 6b). Across species, K_{xc} was also strongly related to anatomical traits. K_{xc} increased positively with the xylem conductances of 1°

© 2025 The Author(s).
New Phytologist © 2025 New Phytologist Foundation.

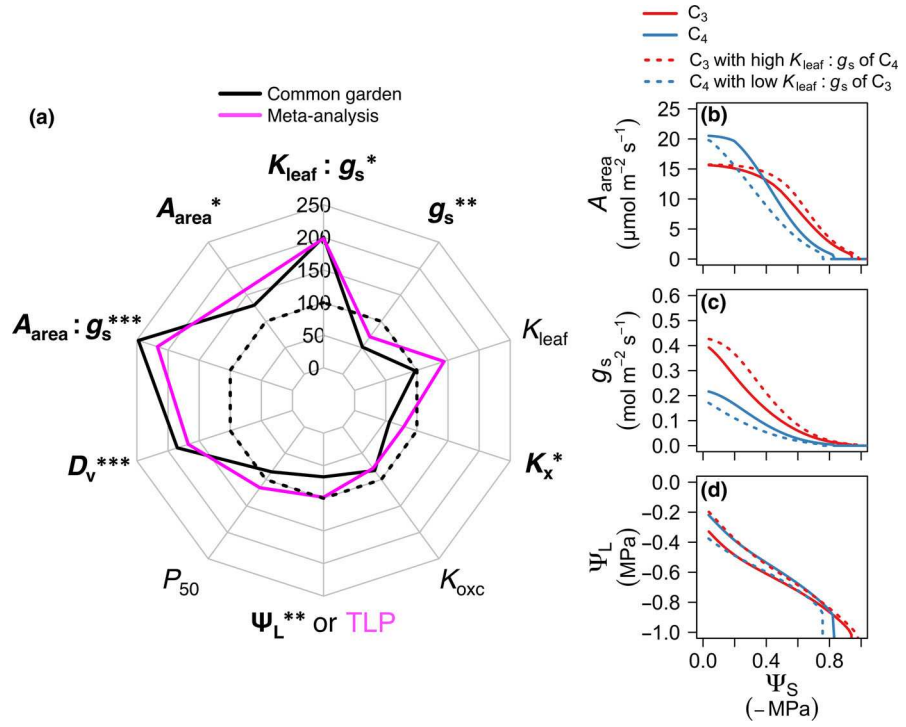

Fig. 3 Contrasting hydraulic and photosynthetic physiology of C_3 and C_4 grasses and modeled impacts of their traits on physiological declines under drought. Leaf hydraulic and photosynthetic traits including the ratio of leaf hydraulic conductance to stomatal conductance (K_{leaf} : g_s), stomatal conductance (g_s), leaf hydraulic conductance (K_{leaf}), leaf xylem conduit hydraulic conductance (K_{xc}), leaf outside-xylem conduit hydraulic conductance (K_{oxc}), leaf water potential (Ψ_L), leaf turgor loss point (TLP), leaf water potential at 50% loss of hydraulic conductivity (P_{50}), leaf vein density (D_v), the ratio of light-saturated photosynthetic rate per leaf area to stomatal conductance (A_{area} : g_s), and light-saturated photosynthetic rate per leaf area (A_{area}) for (a) 27 common garden-grown grasses and 332 grasses from the compiled database, where C_3 species means were fixed arbitrarily as the 100% reference value (dark dashed line), and the black and magenta solid lines indicate the percent difference between the C_3 and C_4 species for the common garden and the meta-analysis, respectively. Traits in bold type differed significantly between C_3 and C_4 species for the 27 phylogenetically matched common garden species (phylogenetic analysis of variance). Modeled responses of (b) A_{area}, (c) g_s and (d) Ψ_L to declining soil water potential (Ψ_S) at vapor pressure deficit (VPD) of 0.5 kPa (simulations for 3 kPa VPD in Supporting Information Fig. S2). Significance: *, $P < 0.05$; **, $P < 0.01$; ***, $P < 0.001$, for phylogenetic analysis of variance. Statistics and parameters are found in Tables S2 and S3. Means for K_{oxc} excluded *Paspalum diltatum* due to it being an outlier (Dixon's test), though differences in C_3 and C_4 were not significant, whether or not this species was included in phylogenetic analysis of variance.

midvein, and 2° large and 3° intermediate longitudinal vein orders (i.e. $K_{xc\text{-vein order}}$; Fig. S3a–c; Table S7), and considering each longitudinal leaf vein order, the vein K_{xc} scaled positively with its CD (Fig. S3m–p; Table S8). K_{xc} increased with higher CD but was independent of CN averaged across vein orders, and of D_v (Fig. 6c; Table S7). The higher D_v of C_4 species was not associated with an advantage in hydraulic capacity (Fig. 6d; Table S7). Although the higher minor D_v of C_4 grasses would contribute to a twofold higher minor vein xylem construction cost (CC_{minor}), the reduction in minor vein CN at similar CD offsets that additional cost (whether cell wall thickness is considered as constant as in Eqn 9, or as proportional to CD with an exponent < 1), leading to an overall $K_{xc\text{-minor}}/CC_{minor}$ similar to that of C_3 species (Table S2).

Among C_3 and C_4 grass species, A_{area} was related to venation and sheath traits, including D_v, IVD, vein surface area per leaf area (VSA_{total}), vein volume per leaf area (VV_{total}), and bundle and mestome sheath volume per leaf area (BSV and MSV; Figs 6e,f, S4; Table S6). Among C_3 grasses, A_{area} was related to the major vein density ($D_{v\text{-major}}$) and vein surface area (VSA_{major}) (Table S6).

Adaptation of leaf hydraulics and gas exchange to climate in grasses

C_4 grasses were native to climates of lower average aridity index (AI) than C_3 grasses (Table S2). Furthermore, climatic associations of leaf hydraulics and gas exchange differed between C_3 and C_4 grasses (Fig. 4). C_3 grasses native to colder and drier climates, that is, lower MAT and MAP, had higher A_{area}, g_s, and K_{leaf} (Fig. 4c–e; Table S9). By contrast, across C_4 grasses, K_{leaf}, g_s, and A_{area} were decoupled from MAP, MAT, PET, and AI, but higher K_{leaf} : g_s and K_{leaf} : A_{area} were associated with environments with higher PET (Fig. 4f,g; Table S9). Across all species, high WUE_i was associated with higher PET and AI (Fig. 4h; Table S9).

Discussion

Our study provides novel evidence of the critical influence of leaf hydraulic anatomy and physiology on photosynthetic function and adaptation to aridity among grasses, highlighting multiple contrasts across levels of organization for C_3 and C_4 grasses. The

© 2025 The Author(s).
New Phytologist © 2025 New Phytologist Foundation.

14698137, 2025, 5, Downloaded from https://nph.onlinelibrary.wiley.com/doi/10.1111/nph.20341 by Csu Los Angeles Jfk Memorial, Wiley Online Library on [29/05/2025]. See the Terms and Conditions (https://onlinelibrary.wiley.com/terms-and-conditions) on Wiley Online Library for rules of use; OA articles are governed by the applicable Creative Commons License

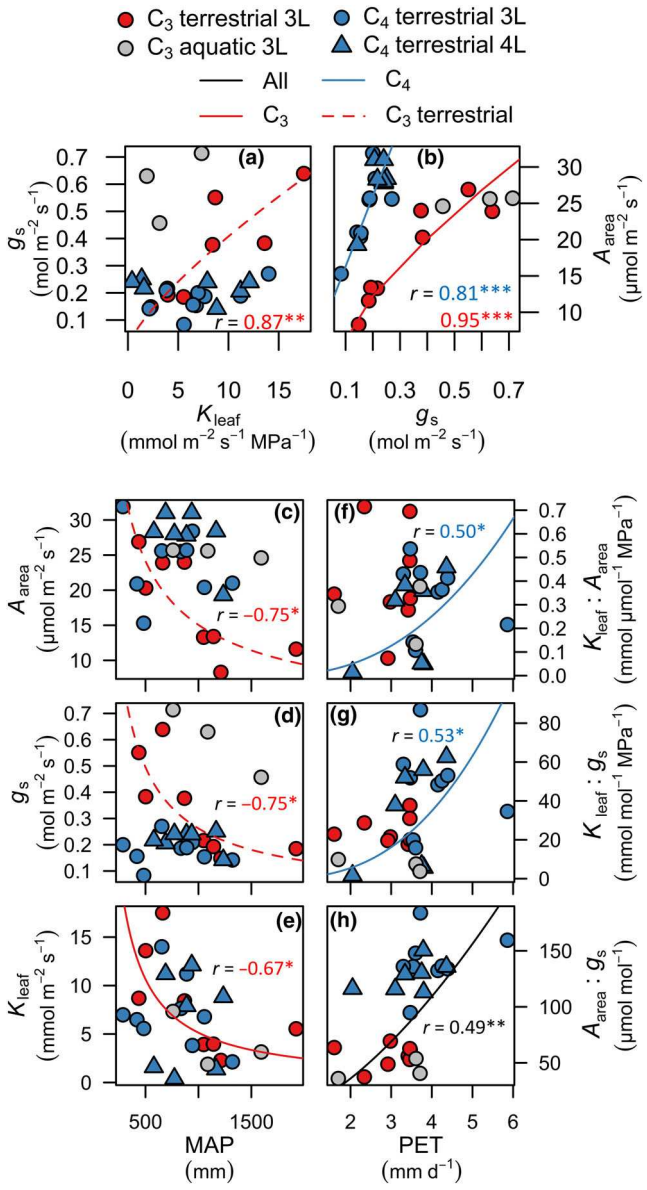

Fig. 4 Contrasting physiological trait coordination and adaptation to aridity in C_3 and C_4 grasses grown in the common garden. Relationships of (a) stomatal conductance (g_s) with leaf hydraulic conductance (K_{leaf}), and of (b) light-saturated leaf photosynthetic rate per leaf area (A_{area}) with g_s. Relationships of (c) A_{area}, (d) g_s, and (e) K_{leaf} with mean annual precipitation (MAP) for only terrestrial C_3 plants in (c, d) and all C_3 in (e), and of (f) the ratio of leaf hydraulic conductance to photosynthetic rate (K_{leaf} : A_{area}) and (g) of the ratio of leaf hydraulic conductance to stomatal conductance (K_{leaf} : g_s) to potential evapotranspiration (PET) for C_4 grasses, and (h) of the ratio of photosynthetic rate to stomatal conductance (A_{area} : g_s, i.e. WUE_i) with PET across all species. Power laws were fitted using phylogenetic reduced major axis regressions (PRMA) for all relationships, except for C_4 species in (b) in which a linear model better characterized this relationship. Red and blue lines indicate that the relationship was significant across C_3 or C_4 species only, respectively, or C_3 and C_4 species with varying slopes, as in (b). Only terrestrial species were included for relationships of C_3 species in (a, c, d). Significance: *, $P < 0.05$; **, $P < 0.01$; ***, $P < 0.001$. $n = 11$ C_3, 16 C_4 species. 3L and 4L in the species key refer to the species having three or four longitudinal vein orders, respectively (Fig. 2). Statistics and parameters are found in Supporting Information Tables S6 and S9.

maintenance of C_4 leaf hydraulic capacity, despite the evolution of lower transpirational demand, leads to a hydraulic surplus and enables stomata to remain open, facilitating the C_4 photosynthetic advantage. This hydraulic surplus leads to contrasting hydraulic and photosynthetic coordination among C_3 and C_4 grasses, resolving paradoxes relating to their vascular anatomy and function, and explains mechanisms of their adaptation to aridity. Our results provide implications for the evolution, ecology, and biogeography of grasses in past and present ecosystems, and applications in agriculture.

The lower g_s and/or higher K_{leaf} of C_4 grasses leads to a disproportionately higher K_{leaf} : g_s in C_4 grasses. Our analyses indicate that this higher K_{leaf} : g_s provides hyper-efficient water transport that is required to achieve higher maximum photosynthetic rates, and enables adaptation to aridity. Hyper-efficient water transport enables higher operating Ψ_{leaf} during gas exchange, maintaining g_s, and resulting in high A_{area} and WUE_i. The high K_{leaf} : g_s of C_4 grasses would be essential to prevent stomatal closure that could obviate much of their C_4 biochemical advantage, as hypothesized previously (Taylor *et al.*, 2010, 2011; Osborne & Sack, 2012). The steeper slope for the relationship of A_{area} and g_s among C_4 grasses is consistent with the C_4 carbon concentrating mechanism eliminating mesophyll resistance limitations on CO_2 assimilation (Bjorkman, 1971) (Figs 4b, 5a), and renders the gas exchange of C_4 species much more sensitive to stomatal closure that would be driven by declining Ψ_{leaf}.

We found contrasting associations of A_{area} and g_s with K_{leaf} among C_3 vs C_4 grasses. For C_3 grasses, the associations of these variables indicate investment in hydraulic supply to match demand and are consistent with that previously observed for A_{area} and K_{leaf} among C_3 grasses, diverse C_3 plant species and species within the C_3 lineage *Viburnum* (Brodribb *et al.*, 2007; Scoffoni *et al.*, 2016; Zhou *et al.*, 2021). Yet, the decoupling of A_{area} and g_s from K_{leaf} among C_4 grasses results from the evolution of consistently lower g_s, which would be selected for in the evolution of C_4. Thus, in C_4 grasses, the evolution of a disproportionate hydraulic supply to demand (K_{leaf} : g_s) leads to decoupling of A_{area} and g_s from K_{leaf}, as has been previously proposed (Zhou *et al.*, 2021).

The determination of leaf hydraulic capacity (K_{leaf}) by the conductance of the outside-xylem pathways (K_{oxc}) can explain paradoxes relating to grass leaf vasculature and hydraulic function. Whereas the higher D_v of C_4 grasses could in theory drive a higher K_{leaf}, the C_4 grasses had higher K_{leaf} only when analyzing the compiled database that included diverse plants grown in different environments, and not in our common garden experiment considering phylogenetically matched species grown in a standardized way. The contrast may thus reflect an influence on the meta-analysis of plasticity in trait values, for example if C_4 grasses would tend to have been experimentally grown or measured in sunnier, warmer conditions. Overall, the determination of K_{leaf} by K_{oxc} rather than K_{xc} indicates that a higher D_v would not drive a higher K_{leaf} through higher K_{xc} across grasses. A higher minor D_v did not even drive a higher K_{xc}, as grasses with higher minor D_v had narrower minor veins containing fewer xylem conduits

© 2025 The Author(s).
New Phytologist © 2025 New Phytologist Foundation.

14698137, 2025, 5, Downloaded from https://nph.onlinelibrary.wiley.com/doi/10.1111/nph.20341 by Csu Los Angeles Jfk Memorial, Wiley Online Library on [29/05/2025]. See the Terms and Conditions (https://onlinelibrary.wiley.com/terms-and-conditions) on Wiley Online Library for rules of use; OA articles are governed by the applicable Creative Commons License

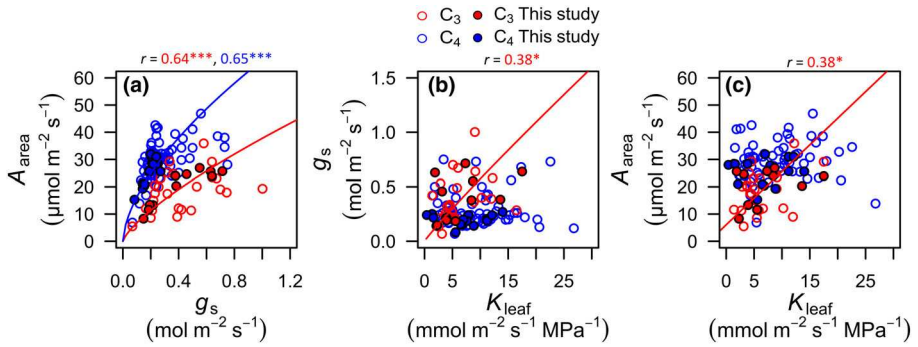

Fig. 5 Coordination of leaf physiological traits across grasses, compiled from published studies (Supporting Information Table S3). Relationships of (a) light-saturated leaf photosynthetic rate (A_{area}) with stomatal conductance (g_s), (b) g_s with leaf hydraulic conductance (K_{leaf}), and (c) A_{area} with K_{leaf}. Lines were fitted with standard major axis (SMA) regressions for log-transformed data in (a) and (b), and for untransformed data in (c), and drawn when significant: *, $P < 0.05$; **, $P < 0.01$; ***, $P < 0.001$. Values were averaged per species across studies, and analyses included data from this study, represented by closed circles in the plots. Statistics and parameters for both ahistorical and phylogenetic regressions for all pairwise combinations of traits are found in Table S5.

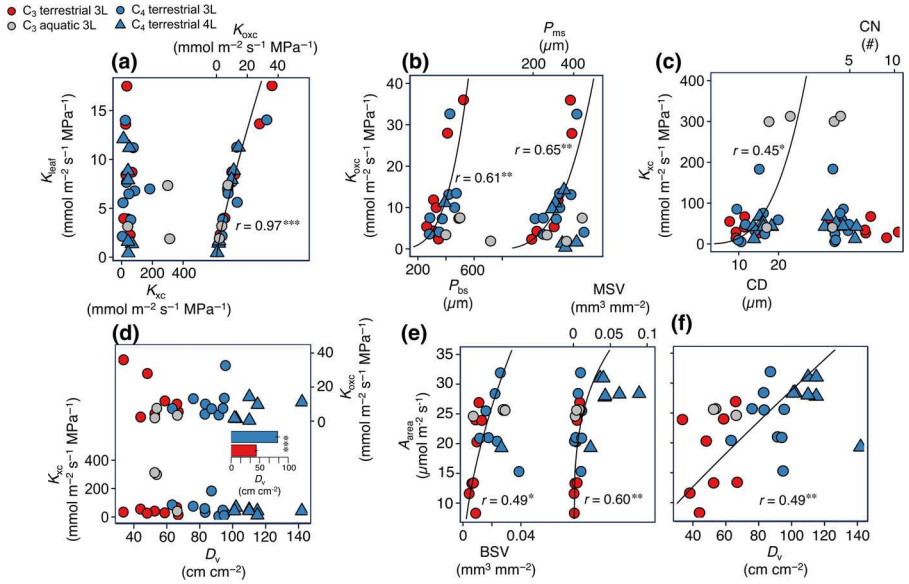

Fig. 6 Anatomical drivers of leaf hydraulic and photosynthetic physiology of C_3 and C_4 grasses. Across 27 C_3 and C_4 grass species grown in a common garden, (a) leaf hydraulic conductance (K_{leaf}) and leaf xylem conduit lumen hydraulic conductance (K_{xc}) were statistically independent, and K_{leaf} was closely related to leaf outside-xylem conduit hydraulic conductance (K_{oxc}). (b) K_{oxc} variation was associated with the perimeters of the vein bundle sheath (P_{bs}) and vein mestome sheath (P_{ms}) tissues. (c) K_{xc} variation was associated with variation in vein conduit diameter (CD) but independent of conduit number (CN). (d) Both K_{xc} and K_{oxc} were independent of vein density (D_v). (e) A higher light-saturated photosynthetic rate (A_{area}) was associated with a higher volume of the bundle sheath (BSV) and mestome sheath (MSV) per leaf area, and (f) D_v. See Supporting Information Table S1 for trait definitions and units. Power laws were fitted using phylogenetic reduced major axis regressions (PRMA) for all relationships across all species, except those in (b) which were significant when considering terrestrial C_3 species and $C_{4\text{-}3L}$ species together. The species *Paspalum dilatatum* was excluded from plots involving K_{oxc} as it was an outlier (Dixon's test), though relationships were significant with or without this species. Significance: *, $P < 0.05$; **, $P < 0.01$; ***, $P < 0.001$. $n = 11$ C_3, 16 C_4 species. Statistics and parameters are found in Tables S6 and S7.

(Fig. S5; Table S10). The low constraint by K_{xc} on K_{leaf} is also consistent with the high efficiency of axial transport through the grass parallel vein architecture relative to radial water transport (Givnish, 1979). A dominant bottleneck in hydraulic transport outside the xylem conduits in grasses is consistent with the low membrane permeability of the bundle sheath (Scoffoni *et al.*, 2023), which may be adaptive for equilibration of water potentials across the mesophyll, and to reduce the tension in the xylem, protecting it from embolism (Cochard *et al.*, 1994; Stiller *et al.*, 2003; Scoffoni *et al.*, 2017, 2023) (Fig. S6). The perimeters of the bundle and mestome sheath tissue layers were correlates of K_{oxc}, highlighting the importance of transport through sheath cell walls thought to be typically highly resistant and hydrophobic and especially through membrane aquaporins and/or

© 2025 The Author(s).
New Phytologist © 2025 New Phytologist Foundation.

14698137, 2025, 5, Downloaded from https://nph.onlinelibrary.wiley.com/doi/10.1111/nph.20341 by Csu Los Angeles Jfk Memorial, Wiley Online Library on [29/05/2025]. See the Terms and Conditions (https://onlinelibrary.wiley.com/terms-and-conditions) on Wiley Online Library for rules of use; OA articles are governed by the applicable Creative Commons License

14698137, 2025, 5, Downloaded from https://nph.onlinelibrary.wiley.com/doi/10.1111/nph.20341 by Csu Los Angeles Jfk Memorial, Wiley Online Library on [29/05/2025]. See the Terms and Conditions (https://onlinelibrary.wiley.com/terms-and-conditions) on Wiley Online Library for rules of use; OA articles are governed by the applicable Creative Commons License

plasmodesmata (Sade *et al.*, 2015; Ohtsuka *et al.*, 2018). Notably, our measurements of K_{leaf} and thus of K_{oxc} are defined for the water pathway ending in the mesophyll protoplasts (Scoffoni *et al.*, 2023); our findings of K_{oxc} being low and dynamic suggest resistant membranes and/or cell walls between the xylem and mesophyll cells. Such a highly resistant membrane and cell wall would be consistent with a recent study reporting airspace subsaturation in C_4 grasses in association with high resistance in the cell membranes and/or cell walls adjacent to the leaf intercellular airspaces (Márquez *et al.*, 2024). In that study, cell membrane resistance was considered a key mechanism enabling stomata to remain hydrated and open and thus avoid a steep decline of A_{area} in C_4 species. That mechanism would operate in parallel with the high K_{leaf} : g_s of C_4 species shown in this study, which would enable leaf water potential to remain high enough to avoid driving stomatal closure. The important role of K_{oxc} in constraining K_{leaf} highlights the need to develop direct measurements of its determinants, for example membrane conductivity.

With respect to xylem conductance, the influence of CD on K_{xc} within and across grass species is consistent with a key role for the large variation in conduit diameters across species, especially the large conduits in the major longitudinal veins (Fig. 2a–c), which accounted for the bulk of K_{xc} (> 98% across species) (Figs S3, S6; Table S2). Our findings suggest very limited constraints by the cost of xylem on the evolution of high D_v for C_4 carbon concentration in grasses. Despite the higher minor D_v of C_4 grasses, given their lower minor vein CN and similar CD to C_3 species, we found that C_3 and C_4 species had similar minor vein xylem hydraulic conductance relative to minor vein xylem construction cost ($K_{xc\text{-}minor}/CC_{minor}$) (Table S2). Our finding for grass leaves thus contrasts with the finding that stems of C_4 eudicots evolved lower hydraulic conductance associated with reduced xylem construction costs (Kocacinar & Sage, 2003, 2004). Shifts in xylem properties may also be linked with mechanical properties that contribute to herbivory resistance and/or optimizing light-use efficiency (Duarte *et al.*, 2023).

The associations between A_{area} and numerous vein and sheath traits provide new mechanistic insights. The influence of high D_v on A_{area} was not mediated directly by hydraulics, as K_{leaf}, K_{xc}, and K_{oxc} were not associated with D_v, $D_{v\text{-}major}$, or VSA_{major}. This finding was consistent with K_{leaf} depending most strongly on high outside-xylem limitation (Fig. 6a). Positive associations between A_{area} and D_v, $D_{v\text{-}major}$, and VSA_{major} may be related to the transport of sugar rather than water, as higher vascularity would reduce transport resistance between veins and mesophyll and provide greater vein sheath surface for exchange, and more parallel transport pathways (Adams *et al.*, 2013). However, across the C_3 species, the relationship of A_{area} with vein sheath traits BSV and MSV may be consistent with a hydraulic basis, arising because the associations of K_{oxc} and K_{leaf} with P_{bs} and P_{ms} enable higher g_s and A_{area} (Tables S6, S7). By contrast, among C_4 grasses, the positive association between A_{area} and BSV and MSV was not mediated by K_{oxc} or K_{leaf}, and arises from contributions to greater volumes of photosynthetic vein sheath tissue (Figs 1, 6; Table S6) (Christin *et al.*, 2013), and because the higher $D_{v\text{-}minor}$ of C_4 species increased BSV and MSV (Table S2).

The higher K_{leaf} : g_s in C_4 grasses and the contrasting coordination of leaf hydraulics and gas exchange for C_3 and C_4 grasses indicate differential mechanisms for adaptation to macroclimate. Our simulations show that a high K_{leaf} : g_s is as necessary as their C_4 biochemistry in providing the photosynthetic advantage of C_4 over C_3 grasses under even mild drought, and therefore is vital to their domination of open, lower rainfall environments (Edwards & Smith, 2010) (Fig. 4g). Notably, a high K_{leaf} : g_s would have been critical for C_4 species to maintain open stomata under the low CO_2 atmosphere experienced during the proliferation of the C_4 grass lineages in the Miocene, and to sustain the high A_{area} that fueled their competitive advantage (Edwards *et al.*, 2010), especially in dry climates, and would also potentially support leaf transpirational cooling in hot environments (Blonder *et al.*, 2023). As C_4 arose repeatedly in grass evolution, along with lower g_s driven by the development of fewer and smaller stomata, a high K_{leaf} : g_s would have evolved repeatedly during the adaptation of high D_v coupled with C_4 vein sheath traits in dry and sunny environments (Sage, 2004; Osborne & Sack, 2012; Taylor *et al.*, 2012; Christin *et al.*, 2013; Zhou & Osborne, 2024). Thus, high K_{leaf} : g_s would have evolved as a precursor adaptation or simultaneously with C_4 biochemistry (Marazzi *et al.*, 2012), and should be considered as a critical target in engineering novel C_4 crop species.

The diversification of C_3 grasses with higher A_{area}, g_s, and K_{leaf} under cold and dry climates is consistent with stress avoidance by capitalizing on short rainfall pulses and growing seasons to compensate for reduced performance during dry and cold periods (Grubb, 1998; Liu *et al.*, 2019). The differential associations of hydraulic and photosynthetic traits with climate in C_3 and C_4 grasses would contribute to their avoidance of drought, that is, their compensating for climatic aridity with rapid growth during the shorter duration of high moisture (Fig. 4). The similar average P_{50} and TLP of C_3 and C_4 species is also consistent with their adaptation to competitive growth when water is available, and adaptation to aridity typically achieved through drought avoidance (Fig. 3a). Notably, adaptation to climate in our study was resolved by testing annual mean macroclimate variables from species' native ranges, which were strongly associated with seasonal mean variables (see Methods S8). We note that species would adapt differently both to seasonality and to different axes of aridity, for example soil and atmospheric drought and their interactions. Indeed, the adaptive trait mechanisms shown here may also be associated with other aspects of ecology, including herbivore susceptibility and flammability, and further disentangling this complexity for trait–climate associations forms a major avenue for future research.

Acknowledgements

We thank T. Cheng, P-A Christin, M. Cilluffo, W. Deng, A. C. Diener, A. Kooner, M. McMaster, S. Moshrefi, L. A. Nikolov, A. J. Patel, V. M. Savage, A. Sayari, and F. Zapata for logistical assistance. This work was funded by the US National Science Foundation grants 1457279, 1951244, 2017949, and 1943583, the UK Natural Environment Research Council grants

© 2025 The Author(s).
New Phytologist © 2025 New Phytologist Foundation.

NE/DO13062/1 and NE/T000759/1, and the Swiss National Science Foundation grant 224221.

Competing interests

None declared.

Author contributions

ASB, SHT, CPO and LS conceptualized the project, developed the methodology, and validated the data. ASB, SHT, JP-K, CV, YZ, TW, HC, CS, EJE, CPO and LS performed the data curation, and reviewed and edited the manuscript. ASB and LS undertook the formal analyses and wrote the original draft. ASB, CS, CPO and LS acquired the funding. ASB, SHT, JP-K, TW, CS, EJE, CPO and LS performed the investigations. ASB, SHT, JP-K, CPO and LS administered and supervised the project. ASB, SHT, JP-K, TW, CS, CPO and LS provided the resources. ASB, SHT and HC wrote the software. ASB and CV provided the data visualization.

ORCID

Alec S. Baird https://orcid.org/0000-0002-9859-5633
Hervé Cochard https://orcid.org/0000-0002-2727-7072
Erika J. Edwards https://orcid.org/0000-0003-0515-2778
Colin P. Osborne https://orcid.org/0000-0002-7423-3718
Lawren Sack https://orcid.org/0000-0002-7009-7202
Christine Scoffoni https://orcid.org/0000-0002-2680-3608
Samuel H. Taylor https://orcid.org/0000-0001-9714-0656
Teera Watcharamongkol https://orcid.org/0000-0002-3065-8597

Data availability

All data are available in Tables S2–S4. Code used for phylogenetic analyses was previously published (Baird *et al.*, 2021) and is available on GitHub (https://github.com/smuel-tylor/grass-leaf-size).

References

Adams W, Cohu C, Muller O, Demmig-Adams B. 2013. Foliar phloem infrastructure in support of photosynthesis. *Frontiers in Plant Science* **4**: 1–8.

Alber M, Petit G, Sellin A. 2019. Does elevated air humidity modify hydraulically relevant anatomical traits of wood in *Betula pendula*? *Trees* **33**: 1361–1371.

Baird AS, Taylor SH, Pasquet-Kok J, Vuong C, Zhang Y, Watcharamongkol T, Scoffoni C, Edwards EJ, Christin P-A, Osborne CP *et al.* 2021. Developmental and biophysical determinants of grass leaf size worldwide. *Nature* **592**: 242–247.

Baird AS, Taylor SH, Reddi S, Pasquet-Kok J, Vuong C, Zhang Y, Watcharamongkol T, John GP, Scoffoni C, Osborne CP *et al.* 2024. Allometries of cell and tissue anatomy and photosynthetic rate across leaves of C_3 and C_4 grasses. *Plant, Cell & Environment* **47**: 156–173.

Beer C, Reichstein M, Tomelleri E, Ciais P, Jung M, Carvalhais N, Rödenbeck C, Arain MA, Baldocchi D, Bonan GB *et al.* 2010. Terrestrial gross carbon dioxide uptake: global distribution and covariation with climate. *Science* **329**: 834–838.

Bellasio C, Stuart-Williams H, Farquhar GD, Flexas J. 2023. C_4 maize and sorghum are more sensitive to rapid dehydration than C_3 wheat and sunflower. *New Phytologist* **240**: 2239–2252.

Bjorkman O. 1971. Interaction between the effects of oxygen and CO_2 concentration on quantum yield and light saturated rate of photosynthesis in the leaves of *Atriplex patula*, ssp. *spicata*. *Carnegie Institution of Washington Year Book* **70**: 520–526.

Blonder B, Aparecido LMT, Hultine KR, Lombardozzi D, Michaletz ST, Posch BC, Slot M, Winter K. 2023. Plant water use theory should incorporate hypotheses about extreme environments: population ecology, and community ecology. *New Phytologist* **238**: 2271–2283.

Bonan G. 2019. *Climate change and terrestrial ecosystem modeling*. Cambridge, UK: Cambridge University Press.

Brodribb TJ, Feild TS, Jordan GJ. 2007. Leaf maximum photosynthetic rate and venation are linked by hydraulics. *Plant Physiology* **144**: 1890–1898.

Brodribb TJ, Jordan GJ. 2008. Internal coordination between hydraulics and stomatal control in leaves. *Plant, Cell & Environment* **31**: 1557–1564.

Buchholz M. 1921. Über die Wasserleitungsbahnen in den interkalaren Wachstumszonen monokotyler Sprosse. *Flora* **114**: 119–186.

von Caemmerer S. 2000. *Biochemical Models of Leaf Photosynthesis*. Collingwood, Vic., Australia: CSIRO.

von Caemmerer S. 2021. Updating the steady-state model of C_4 photosynthesis. *Journal of Experimental Botany* **72**: 6003–6017.

von Caemmerer S, Evans JR. 2010. Enhancing C_3 photosynthesis. *Plant Physiology* **154**: 589–592.

Canny MJ. 2001. Embolisms and refilling in the maize leaf lamina, and the role of the protoxylem lacuna. *American Journal of Botany* **88**: 47–51.

Christin P-A, Osborne CP, Chatelet DS, Columbus JT, Besnard G, Hodkinson TR, Garrison LM, Vorontsova MS, Edwards EJ. 2013. Anatomical enablers and the evolution of C_4 photosynthesis in grasses. *Proceedings of the National Academy of Sciences, USA* **110**: 1381–1386.

Cochard H, Ewers FW, Tyree MT. 1994. Water relations of a tropical vine-like bamboo (*Rhipidocladum racemiflorum*): root pressures, vulnerability to cavitation and seasonal changes in embolism. *Journal of Experimental Botany* **45**: 1085–1089.

Cochard H, Nardini A, Coll L. 2004. Hydraulic architecture of leaf blades: where is the main resistance? *Plant, Cell & Environment* **27**: 1257–1267.

Cochard H, Pimont F, Ruffault J, Martin-StPaul N. 2021. SurEau: a mechanistic model of plant water relations under extreme drought. *Annals of Forest Science* **78**: 1–23.

Cordell S, Goldstein G, Mueller-Dombois D, Webb D, Vitousek PM. 1998. Physiological and morphological variation in *Metrosideros polymorpha*, a dominant Hawaiian tree species, along an altitudinal gradient: the role of phenotypic plasticity. *Oecologia* **113**: 188–196.

Duarte MA, Woo S, Hultine K, Blonder B, Aparecido LMT. 2023. Vein network redundancy and mechanical resistance mitigate gas exchange losses under simulated herbivory in desert plants. *AoB Plants* **15**: plad002.

Edwards EJ, Osborne CP, Strömberg CAE, Smith SA, C4 Grasses Consortium, Bond WJ, Christin P-A, Cousins AB, Duvall MR, Fox DL *et al.* 2010. The origins of C_4 grasslands: integrating evolutionary and ecosystem science. *Science* **328**: 587–591.

Edwards EJ, Smith SA. 2010. Phylogenetic analyses reveal the shady history of C_4 grasses. *Proceedings of the National Academy of Sciences, USA* **107**: 2532–2537.

Evert RF. 2006. *Esau's plant anatomy: meristems, cells, and tissues of the plant body: their structure, function, and development*. Hoboken, NJ: John Wiley.

Fletcher LR, Scoffoni C, Farrell C, Buckley TN, Pellegrini M, Sack L. 2022. Testing the association of relative growth rate and adaptation to climate across natural ecotypes of *Arabidopsis*. *New Phytologist* **236**: 413–432.

Freckleton RP, Harvey PH, Pagel M. 2002. Phylogenetic analysis and comparative data: a test and review of evidence. *The American Naturalist* **160**: 712–726.

Funk JL, Rakovski CS, Macpherson JM. 2015. On the analysis of phylogenetically paired designs. *Ecology and Evolution* **5**: 940–947.

Garland T Jr, Dickerman AW, Janis CM, Jones JA. 1993. Phylogenetic analysis of covariance by computer simulation. *Systematic Biology* **42**: 265–292.

Ghannoum O, Conroy JP, Driscoll SP, Paul MJ, Foyer CH, Lawlor DW. 2003. Nonstomatal limitations are responsible for drought-induced photosynthetic inhibition in four C_4 grasses. *New Phytologist* **159**: 599–608.

© 2025 The Author(s).
New Phytologist © 2025 New Phytologist Foundation.

14698137, 2025, 5, Downloaded from https://nph.onlinelibrary.wiley.com/doi/10.1111/nph.20341 by Csu Los Angeles Jfk Memorial, Wiley Online Library on [29/05/2025]. See the Terms and Conditions (https://onlinelibrary.wiley.com/terms-and-conditions) on Wiley Online Library for rules of use; OA articles are governed by the applicable Creative Commons License

Givnish T. 1979. On the adaptive significance of leaf form. In: Solbrig OT, Jain S, Johnson GB, Raven PH, eds. *Topics in plant population biology*. London, UK: Macmillan Education UK, 375–407.

Givnish T, Montgomery RA. 2014. Common-garden studies on adaptive radiation of photosynthetic physiology among Hawaiian lobeliads. *Proceedings of the Royal Society B: Biological Sciences* **281**: 20132944.

Gleason SM, Blackman CJ, Chang Y, Cook AM, Laws CA, Westoby M. 2016. Weak coordination among petiole, leaf, vein, and gas-exchange traits across Australian angiosperm species and its possible implications. *Ecology and Evolution* **6**: 267–278.

Gowik U, Westhoff P. 2011. The path from C_3 to C_4 photosynthesis1. *Plant Physiology* **155**: 56–63.

Grass Phylogeny Working Group II. 2012. New grass phylogeny resolves deep evolutionary relationships and discovers C_4 origins. *New Phytologist* **193**: 304–312.

Grubb PJ. 1998. A reassessment of the strategies of plants which cope with shortages of resources. *Perspectives in Plant Ecology, Evolution and Systematics* **1**: 3–31.

Higgins SI, Scheiter S. 2012. Atmospheric CO_2 forces abrupt vegetation shifts locally, but not globally. *Nature* **488**: 209–212.

Hodgson D, McDonald JL, Hosken DJ. 2015. What do you mean, 'resilient'? *Trends in Ecology & Evolution* **30**: 503–506.

Holloway-Phillips M-M, Brodribb TJ. 2011. Minimum hydraulic safety leads to maximum water-use efficiency in a forage grass. *Plant, Cell & Environment* **34**: 302–313.

Huxman TE, Winkler DE, Mooney KA. 2022. A common garden super-experiment: an impossible dream to inspire possible synthesis. *Journal of Ecology* **110**: 997–1004.

Jacob V, Choat B, Churchill AC, Zhang H, Barton CVM, Krishnananthaselvan A, Post AK, Power SA, Medlyn BE, Tissue DT. 2022. High safety margins to drought-induced hydraulic failure found in five pasture grasses. *Plant, Cell & Environment* **45**: 1631–1646.

Kocacinar F, Sage RF. 2003. Photosynthetic pathway alters xylem structure and hydraulic function in herbaceous plants. *Plant, Cell & Environment* **26**: 2015–2026.

Kocacinar F, Sage RF. 2004. Photosynthetic pathway alters hydraulic structure and function in woody plants. *Oecologia* **139**: 214–223.

Langdale JA. 2011. C_4 cycles: past, present, and future research on C_4 photosynthesis. *Plant Cell* **23**: 3879–3892.

Lewis AM, Boose ER. 1995. Estimating volume flow rates through xylem conduits. *American Journal of Botany* **82**: 1112–1116.

Liu H, Taylor SH, Xu Q, Lin Y, Hou H, Wu G, Ye Q. 2019. Life history is a key factor explaining functional trait diversity among subtropical grasses, and its influence differs between C_3 and C_4 species. *Journal of Experimental Botany* **70**: 1567–1580.

Marazzi B, Ané C, Simon MF, Delgado-Salinas A, Luckow M, Sanderson MJ. 2012. Locating evolutionary precursors on a phylogenetic tree. *Evolution* **66**: 3918–3930.

Márquez DA, Wong SC, Stuart-Williams H, Cernusak LA, Farquhar GD. 2024. Mesophyll airspace unsaturation drives C_4 plant success under vapor pressure deficit stress. *Proceedings of the National Academy of Sciences, USA* **121**: 1–9.

Martre P, Cochard H, Durand J-L. 2001. Hydraulic architecture and water flow in growing grass tillers (*Festuca arundinacea* Schreb.). *Plant, Cell & Environment* **24**: 65–76.

Martre P, Durand J. 2001. Quantitative analysis of vasculature in the leaves of *Festuca arundinacea* (Poaceae): implications for axial water transport. *International Journal of Plant Sciences* **162**: 755–766.

Martre P, Durand J-L, Cochard H. 2000. Changes in axial hydraulic conductivity along elongating leaf blades in relation to xylem maturation in tall fescue. *New Phytologist* **146**: 235–247.

Matos IS, McDonough S, Carrillo Johnson B, Kalantar D, Rohde J, Sahu R, Wang J, Fontao A, To J, Carlos S *et al.* 2024. Negative allometry of leaf xylem conduit diameter and double-wall thickness: implications for implosion safety. *New Phytologist* **242**: 2464–2478.

McKown AD, Cochard H, Sack L. 2010. Decoding leaf hydraulic with a spatially explicit model: Principles of venation architecture and implications for its evolution. *American Naturalist* **175**: 447–460.

McSteen P, Kellogg EA. 2022. Molecular, cellular, and developmental foundations of grass diversity. *Science* **377**: 599–602.

Meinzer FC, Goldstein G, Neufeld HS, Grantz DA, Crisosto GM. 1992. Hydraulic architecture of sugarcane in relation to patterns of water use during plant development. *Plant, Cell & Environment* **15**: 471–477.

Mertz RA, Brutnell TP. 2014. Bundle sheath suberization in grass leaves: multiple barriers to characterization. *Journal of Experimental Botany* **65**: 3371–3380.

Nobel PS. 2020. *Physicochemical and environmental plant physiology*. San Diego, CA, USA: Academic Press.

North GB, Browne MG, Fukui K, Maharaj FDR, Phillips CA, Woodside WT. 2016. A tale of two plasticities: leaf hydraulic conductances and related traits diverge for two tropical epiphytes from contrasting light environments. *Plant, Cell & Environment* **39**: 1408–1419.

Ocheltree TW, Nippert JB, Prasad PVV. 2014. Stomatal responses to changes in vapor pressure deficit reflect tissue-specific differences in hydraulic conductance. *Plant, Cell & Environment* **37**: 132–139.

Ocheltree TW, Nippert JB, Prasad PVV. 2016. A safety vs efficiency trade-off identified in the hydraulic pathway of grass leaves is decoupled from photosynthesis, stomatal conductance and precipitation. *New Phytologist* **210**: 97–107.

Ogle K. 2003. Implications of interveinal distance for quantum yield in C_4 grasses: a modeling and meta-analysis. *Oecologia* **136**: 532–542.

Ohtsuka A, Sack L, Taneda H. 2018. Bundle sheath lignification mediates the linkage of leaf hydraulics and venation. *Plant, Cell & Environment* **41**: 342–353.

Osborne CP, Freckleton RP. 2009. Ecological selection pressures for C_4 photosynthesis in the grasses. *Proceedings of the Royal Society B: Biological Sciences* **276**: 1753–1760.

Osborne CP, Sack L. 2012. Evolution of C_4 plants: a new hypothesis for an interaction of CO_2 and water relations mediated by plant hydraulics. *Philosophical Transactions of the Royal Society of London. Series B: Biological Sciences* **367**: 583–600.

Pagel M. 1999. Inferring the historical patterns of biological evolution. *Nature* **401**: 877–884.

Pasquet-Kok J, Creese C, Sack L. 2010. Turning over a new 'leaf': multiple functional significances of leaves versus phyllodes in Hawaiian *Acacia koa*. *Plant, Cell & Environment* **33**: 2084–2100.

Pathare VS, Sonawane BV, Koteyeva N, Cousins AB. 2020. C_4 grasses adapted to low precipitation habitats show traits related to greater mesophyll conductance and lower leaf hydraulic conductance. *Plant, Cell & Environment* **43**: 1897–1910.

Pinheiro J, Bates D, Debroy S, Sarkar D. 2019. *NLME: linear and nonlinear mixed effect models*. R package version 3.1-140. [WWW document] URL https://CRAN.R-project.org/package=nlme.

R Core Team. 2023. *R: a language and environment for statistical computing*. Vienna, Austria: R Foundation for Statistical Computing.

Revell LJ. 2012. PHYTOOLS: an R package for phylogenetic comparative biology (and other things). *Methods in Ecology and Evolution* **3**: 217–223.

Sack L, Frole K. 2006. Leaf structural diversity is related to hydraulic capacity in tropical rain forest trees. *Ecology* **87**: 483–491.

Sack L, Holbrook NM. 2006. Leaf hydraulics. *Annual Review of Plant Biology* **57**: 361–381.

Sack L, Scoffoni C. 2012. Measurement of leaf hydraulic conductance and stomatal conductance and their responses to irradiance and dehydration using the evaporative flux method (EFM). *Journal of Visualized Experiments* **4179**: 1–7.

Sack L, Scoffoni C. 2013. Leaf venation: structure, function, development, evolution, ecology and applications in the past, present and future. *New Phytologist* **198**: 983–1000.

Sade N, Shatil-Cohen A, Moshelion M. 2015. Bundle-sheath aquaporins play a role in controlling Arabidopsis leaf hydraulic conductivity. *Plant Signaling & Behavior* **10**: e1017177.

Sage RF. 2004. The evolution of C_4 photosynthesis. *New Phytologist* **161**: 341–370.

Sage RF, Christin P-A, Edwards EJ. 2011. The C_4 plant lineages of planet earth. *Journal of Experimental Botany* **62**: 3155–3169.

© 2025 The Author(s).
New Phytologist © 2025 New Phytologist Foundation.

14698137, 2025, 5, Downloaded from https://nph.onlinelibrary.wiley.com/doi/10.1111/nph.20341 by Csu Los Angeles Jfk Memorial, Wiley Online Library on [29/05/2025]. See the Terms and Conditions (https://onlinelibrary.wiley.com/terms-and-conditions) on Wiley Online Library for rules of use; OA articles are governed by the applicable Creative Commons License

Schrader J, Shi P, Royer DL, Peppe DJ, Gallagher RV, Li Y, Wang R, Wright IJ. 2021. Leaf size estimation based on leaf length, width and shape. *Annals of Botany* **128**: 395–406.

Scoffoni C, Albuquerque C, Brodersen CR, Townes SV, John GP, Bartlett MK, Buckley TN, McElrone AJ, Sack L. 2017. Outside-xylem vulnerability, not xylem embolism, controls leaf hydraulic decline during dehydration. *Plant Physiology* **173**: 1197–1210.

Scoffoni C, Albuquerque C, Buckley TN, Sack L. 2023. The dynamic multi-functionality of leaf water transport outside the xylem. *New Phytologist* **239**: 2099–2107.

Scoffoni C, Chatelet DS, Pasquet-kok J, Rawls M, Donoghue MJ, Edwards EJ, Sack L. 2016. Hydraulic basis for the evolution of photosynthetic productivity. *Nature Plants* **2**: 1–8.

Scoffoni C, McKown AD, Rawls M, Sack L. 2012. Dynamics of leaf hydraulic conductance with water status: quantification and analysis of species differences under steady state. *Journal of Experimental Botany* **63**: 643–658.

Sexton JP, McIntyre PJ, Angert AL, Rice KJ. 2009. Evolution and ecology of species range limits. *Annual Review of Ecology, Evolution, and Systematics* **40**: 415–436.

Shi P, Liu M, Ratkowsky DA, Gielis J, Su J, Yu X, Wang P, Zhang L, Lin Z, Schrader J. 2019. Leaf area–length allometry and its implications in leaf shape evolution. *Trees* **33**: 1073–1085.

Sommerville KE, Sack L, Ball MC. 2012. Hydraulic conductance of *Acacia* phyllodes (foliage) is driven by primary nerve (vein) conductance and density. *Plant, Cell & Environment* **35**: 158–168.

Sonawane BV, Koteyeva NK, Johnson DM, Cousins AB. 2021. Differences in leaf anatomy determines temperature response of leaf hydraulic and mesophyll CO_2 conductance in phylogenetically related C_4 and C_3 grass species. *New Phytologist* **230**: 1802–1814.

Spriggs EL, Christin P-A, Edwards EJ. 2014. C_4 photosynthesis promoted species diversification during the miocene grassland expansion. *PLoS ONE* **9**: e97722.

Stiller V, Lafitte HR, Sperry JS. 2003. Hydraulic properties of rice and the response of gas exchange to water stress. *Plant Physiology* **132**: 1698–1706.

Taylor SH, Aspinwall MJ, Blackman CJ, Choat B, Tissue DT, Ghannoum O. 2018. CO_2 availability influences hydraulic function of C_3 and C_4 grass leaves. *Journal of Experimental Botany* **69**: 2731–2741.

Taylor SH, Franks PJ, Hulme SP, Spriggs E, Christin PA, Edwards EJ, Woodward FI, Osborne CP. 2012. Photosynthetic pathway and ecological adaptation explain stomatal trait diversity amongst grasses. *New Phytologist* **193**: 387–396.

Taylor SH, Hulme SP, Rees M, Ripley BS, Ian Woodward F, Osborne CP. 2010. Ecophysiological traits in C_3 and C_4 grasses: a phylogenetically controlled screening experiment. *New Phytologist* **185**: 780–791.

Taylor SH, Ripley BS, Martin T, De-Wet L-A, Woodward FI, Osborne CP. 2014. Physiological advantages of C_4 grasses in the field: a comparative experiment demonstrating the importance of drought. *Global Change Biology* **20**: 1992–2003.

Taylor SH, Ripley BS, Woodward FI, Osborne CP. 2011. Drought limitation of photosynthesis differs between C_3 and C_4 grass species in a comparative experiment. *Plant, Cell & Environment* **34**: 65–75.

Ueno O, Kawano Y, Wakayama M, Takeda T. 2006. Leaf vascular systems in C_3 and C_4 grasses: a two-dimensional analysis. *Annals of Botany* **97**: 611–621.

Volaire F. 2018. A unified framework of plant adaptive strategies to drought: crossing scales and disciplines. *Global Change Biology* **24**: 2929–2938.

Warton DI, Duursma RA, Falster DS, Taskinen S. 2012. SMATR 3 – an R package for estimation and inference about allometric lines. *Methods in Ecology and Evolution* **3**: 257–259.

Weitz JS, Ogle K, Horn HS. 2006. Ontogenetically stable hydraulic design in woody plants. *Functional Ecology* **20**: 191–199.

Xiong D, Flexas J, Yu T, Peng S, Huang J. 2017. Leaf anatomy mediates coordination of leaf hydraulic conductance and mesophyll conductance to CO_2 in *Oryza*. *New Phytologist* **213**: 572–583.

Yin X, Sun Z, Struik PC, Van Der Putten PEL, Van Ieperen W, Harbinson J. 2011. Using a biochemical C_4 photosynthesis model and combined gas exchange and chlorophyll fluorescence measurements to estimate bundle-sheath conductance of maize leaves differing in age and nitrogen content. *Plant, Cell & Environment* **34**: 2183–2199.

Zhou H, Akçay E, Edwards E, Helliker B. 2021. The legacy of C_4 evolution in the hydraulics of C_3 and C_4 grasses. *bioRxiv*. doi: 10.1101/2020.05.14.097030.

Zhou Y, Osborne CP. 2024. Stomatal dynamics in *Alloteropsis semialata* arise from the evolving interplay between photosynthetic physiology, stomatal size and biochemistry. *Plant, Cell & Environment* **47**: 4586–4598.

Supporting Information

Additional Supporting Information may be found online in the Supporting Information section at the end of the article.

Fig. S1 Phylogenetic tree and biogeographic distributions of 27 grass species grown in a common garden and sampled for hydraulic and anatomical traits.

Fig. S2 Results of simulation modeling of the hydraulic-stomatal-photosynthetic system of C_3 and C_4 grasses.

Fig. S3 Coordination of leaf photosynthetic rate with leaf hydraulic anatomy.

Fig. S4 Testing determinants of leaf xylem conduit hydraulic conductance (K_{xc}).

Fig. S5 Relationships of 3° leaf hydraulic conductance and vein traits in C_4 grasses.

Fig. S6 Partitioning of the leaf hydraulic resistance and leaf xylem conductance across vein orders.

Methods S1 Plant growth conditions.

Methods S2 Preparation of leaf transverse cross sections.

Methods S3 Quantification of leaf hydraulic conductance.

Methods S4 Quantification of leaf gas exchange.

Methods S5 Vein order categorization for anatomy measurements.

Methods S6 Details on the calculation of leaf xylem conduit hydraulic conductance.

Methods S7 Quantification of additional potential correlates of leaf outside-xylem conduit hydraulic conductance.

Methods S8 Modeling the native climate of C_3 and C_4 grasses.

Methods S9 Details on functions and approaches used for statistical analyses.

Methods S10 Modeling of hydraulic-stomatal-photosynthetic function of C_3 and C_4 species during drought and varying vapor pressure deficit.

© 2025 The Author(s).
New Phytologist © 2025 New Phytologist Foundation.

14698137, 2025, 5, Downloaded from https://nph.onlinelibrary.wiley.com/doi/10.1111/nph.20341 by Csu Los Angeles Jfk Memorial, Wiley Online Library on [29/05/2025]. See the Terms and Conditions (https://onlinelibrary.wiley.com/terms-and-conditions) on Wiley Online Library for rules of use; OA articles are governed by the applicable Creative Commons License

Table S1 Variables quantified for C_3 and C_4 grass species: leaf hydraulic physiology, gas exchange physiology, venation and structure and vein sheath anatomy.

Table S2 Species of grasses (Poaceae) included in the common garden study, subfamily, tribe, C_3/C_4 photosynthetic pathway, C_4 subtype, seed source, accession number, seed treatment for germination, terrestrial/aquatic, sun/shade, and mean, ±SE of anatomical and morphological traits measured and climate data, and statistics from phylogenetic analysis of variance below trait means.

Table S3 Hydraulic, photosynthetic and anatomical data for 332 grass species from published studies and used to test relationships of leaf gas exchange and hydraulics across species, and to test average differences between C_3 and C_4 species.

Table S4 Model parameters used to test the importance of high ratio of leaf hydraulic conductance to stomatal conductance (K_{leaf} : g_s) for C_4 photosynthetic advantage in wet and drying soil.

Table S5 Correlation matrices for trait–trait relationships for the 332 grass species database.

Table S6 Statistics and parameters for associations of leaf photosynthetic traits with leaf hydraulic and anatomical traits across all species, terrestrial species only, C_3 species only, C_3 terrestrial species only and C_4 species only, from the common garden.

Table S7 Statistics and parameters for associations of leaf hydraulic traits with leaf hydraulic, photosynthetic and anatomical traits across all species, terrestrial species only, C_3 species only, C_3 terrestrial species only and C_4 species only, from the common garden.

Table S8 Statistics and parameters for associations of leaf xylem hydraulic conductance per vein order with leaf hydraulic anatomy across all species from the common garden.

Table S9 Statistics and parameters for associations of climate with leaf hydraulic, photosynthetic and anatomical traits across all species, terrestrial species only, C_3 species only, C_3 terrestrial species only and C_4 species only, from the common garden.

Table S10 Statistics and parameters for coordination or tradeoffs of leaf structural traits across all species from the common garden.

Please note: Wiley is not responsible for the content or functionality of any Supporting Information supplied by the authors. Any queries (other than missing material) should be directed to the *New Phytologist* Central Office.

Disclaimer: The New Phytologist Foundation remains neutral with regard to jurisdictional claims in maps and in any institutional affiliations.

14698137, 2025, 5, Downloaded from https://nph.onlinelibrary.wiley.com/doi/10.1111/nph.20341 by Csu Los Angeles Jfk Memorial, Wiley Online Library on [29/05/2025]. See the Terms and Conditions (https://onlinelibrary.wiley.com/terms-and-conditions) on Wiley Online Library for rules of use; OA articles are governed by the applicable Creative Commons License

© 2025 The Author(s).
New Phytologist © 2025 New Phytologist Foundation.